(KO) to OXA- or TNBS-induced colitis, 2 representative colitis models for IBD. CD30LKO mice were highly susceptibile to OXA-induced colitis but resistant to TNBS-induced acute colitis. In vivo administration of agonistic anti-CD30 monoclonal antibody (mAb) ameliorated OXA-induced colitis but aggravated TNBS-induced acute colitis in CD30LKO mice. These results suggest that CD30L is involved in development of both types of IBD. Implications of these findings for a novel biologic therapy in controlling IBD are discussed.

## Materials and Methods

### *Mice*

Age- and sex-matched BALB/c or C57BL/6 male mice were obtained from Charles River Laboratories (Atsugi, Japan). The generation of CD30LKO mice with BALB/c background were described previously.[32,33] CD30LKO mice with C57BL/6 background were backcrossed into C57BL/6 mice more than 8 times, and their littermates were used as control. This study was approved by the Committee of Ethics on Animal Experiment in Faculty of Medicine, Kyushu University.



### *Induction of Colitis*

Colitis was induced by intrarectal administration of OXA or TNBS according to the methods described previously.[13,16] Briefly, mice were anesthetized with diethyl ether (Nacalai Tesque, Inc, Kyoto, Japan) and then administered TNBS (3 mg, Sigma–Aldrich Japan Co, Tokyo, Japan) or OXA (0.8% or 1%, 4-ethocymethylene-2-phenyl-2- oxazolin-5-one) (Sigma Chemical Co, St Louis, MO) dissolved in 45% ethanol intrarectally via a 3.5-French catheter equipped with a 1-mL syringe. The catheter was inserted so that the tip was 4 cm proximal to the anal verge, and the haptenating agent was injected with a total volume of 150 $\mu$L. To ensure distribution within the entire colon and cecum, mice were held in a vertical position for 30 seconds after the injection. Control mice were administered an ethanol solution without haptenating agent using the same technique.

### *Histology Assessment of Colitis*

The middle parts of colons were removed and fixed with 10% neutral buffered formalin and then embedded in paraffin. After cutting in round slices, the thin tissue sections were stained with H&E. Histology was scored as follows: epithelium (E): 0, normal morphology; 1, loss of globlet cells; 2, loss of globlet cells in large areas; 3, loss of crypts; 4, loss of crypts in large areas; and infiltration (I): 0, no infiltrate; 1, infiltrate around the crypt basis; 2, infiltrate reaching the L muscularis mucosae; 3, extensive infiltration reaching the L muscularis mucosae and thickening of the mucosa with abundant edema; 4, infiltration of the L submucosa.[34] The total histologic score was given as E + I.

### *Antibodies and Reagents*

FITC-conjugated anti-CD3$\varepsilon$, anti-CD4, anti-CD11c, anti-NK (DX5), anti-CD11b, anti-Foxp3, anti-CD25, and anti-IL-10 mAbs; PE-conjugated anti-Ly-6G, anti-CD30L, anti-CD30, anti-CD8$\alpha$, anti-CD4, anti-CD25, anti-IFN-$\gamma$, anti-IL-10, and anti-IL-4 mAbs; allophycocyanin (APC)-conjugated anti-CD3$\varepsilon$ and anti-CD44 mAbs; and biotin-conjugated anti-F4/80 (BM8) and anti-CD30L and APC-conjugated streptavidin (SA-APC) mAbs were purchased from e-Bioscience (San Diego, CA). PE-conjugated anti-TCR$\gamma\delta$ (GL-3) mAb and PerCP-Cy5.5-labeled anti-CD4 were purchased from BD PharMingen (San Diego, CA). Armenian Hamster IgG1 was purchased from Wako Pure Chemicals (Osaka, Japan).

### *In Vivo Treatment of Mice With Abs*

Agonistic anti-CD30 mAb (clone 30.1) and rat anti-mouse IL-4 (clone 11B11) mAb were obtained by growing hybridoma cells in CELLine CL-1000 (BD, Biosciences, San Diego, CA) with serum-free medium (medium 101; Nissui Pharmaceutical, Tokyo, Japan) and collecting these antibodies by HiTrap Protein G HP (Amersham Biosciences). The purity of the preparation was confirmed by SDS-PAGE, and the concentration of Ab was determined by the Lowry method. The mAbs, diluted to 1 mg/mL in phosphate-buffered saline (PBS), were stored at −70°C until use. For in vivo neutralization, various doses of rat anti-mouse IL-4 or isotype control (rat IgG; e-Bioscience) were intraperitoneally (IP) injected into mice at the time of disease induction with OXA. For in vivo activation, 100 $\mu$g agonistic anti-CD30 mAb or isotype control (hamster IgG1; BD Biosciences) was injected IP into mice before or after induction of colitis.

### *Flow Cytometry Analysis and Intracellular Cytokine Synthesis Analysis*

Lamina propria (LP) cells in the large intestine were isolated by a modified method described previously.[34] LP lymphocytes (LPLs) were purified on a 45%/66.6% discontinuous Percoll (Pharmacia, Uppsala, Sweden) gradient at 600*g* for 20 minutes. For flow cytometry analysis, isolated cells were preincubated with an Fc$\gamma$ receptor-blocking mAb (CD16/32; 2.4G2) for 15 minutes at 4°C then incubated with saturating amounts of FITC-, PE-, APC-, and biotin-conjugated mAbs for 30 minutes at 4°C. To detect biotin-conjugated mAb, cells were stained with APC-conjugated streptavidin, and the stained cells were analyzed by using a FACS Calibur flow cytometer (Becton Dickinson, Mountain View, CA). For intracellular cytokine staining, $10^6$ LP cells were simulated with phorbol myristate acetate (PMA) and ionomycin for 5 hours at 37°C. Brefeldin A (10 $\mu$g/mL; Sigma Chemical Co) was included during the final 4 hours of stimulation. These cells were harvested, washed, and incubated for 30 min at 4°C with mAbs for surface staining then cells were

subjected to intracellular cytokine staining using the Fast Immune Cytokine System according to the manufacturer's instructions (Becton Dickinson Co). The data were analyzed with CellQuest software (BD Biosciences).

### *Culture of LP Cells for Assay of Cytokine Production*

To measure cytokine production by LP cells, $10^6$ LP cells from mice were cultured without any stimulation for 24 hours at 37°C under 5% $CO_2$ in 96-well flat-bottomed plates in a volume of 0.2 mL RPMI containing 10% fetal bovine serum (FBS). For cytokine production by LPT cells, LP cells purified as described above were loaded into uncoated culture wells or wells coated with 10 μg/mL anti-CD3ε mAb and 1 μg/mL soluble anti-CD28 mAb and cultured for 48 hours. The culture supernatants were then harvested and assayed for cytokine concentration by enzyme-linked immunosorbent assay (ELISA) using an ELISA Development Kit (Genzyme Diagnostics, Cambridge, MA).

### *Statistical Analysis*

The difference in survival rates was evaluated by the log-rank test (Mantel–Cox). Disease activity index and histologic scores were statistically analyzed using the Mann–Whitney *U* test. Differences in parametric data were evaluated by Student *t* test. Differences of $P < .05$ were considered statistically significant.

## Results

### *CD30LKO Mice Are Susceptible to OXA-Induced Colitis*

To examine the role of CD30L in development of OXA-induced colitis in mice, CD30LKO mice with BALB/c background were subjected to induction of colitis by intrarectal administration of 1.0% or 0.8% OXA. We first examined the expression levels of CD30L and CD30 on LPL in the colon from naive mice and mice with colitis. The CD30L was expressed mainly on a part of $CD4^+$ T cells from freshly isolated LPL in naive BALB/c mice and mice treated with 0.8% OXA 4 days previously (see Supplemental Figure 1*A* and 1*B* online at www.gastrojournal.org). Although the CD30 expression was not detected on freshly isolated LPL cells in the colon of naïve mice or OXA-treated mice (data not shown), appreciable numbers of $CD30^+$ cells were detected in the $CD4^+$ T-cell population from naïve and OXA-treated mice after 24-hour in vitro culture with or without anti-CD3 mAb stimulation (see Supplemental Figure 1*C* online at www.gastrojournal.org).

The survival rates were significantly decreased in CD30LKO mice compared with those in WT mice after 1% OXA administration (Figure 1*A*, $*P < .05$). CD30LKO mice showed exacerbated colitis as indicated by the significant weight loss from day 3 to day 10 after 0.8% OXA administration (Figure 1*B*, $*P < .05$). Macroscopic examinations on day 2 after 0.8% OXA administration revealed that the colon was shorter in CD30LKO mice than that in WT mice (Figure 1*C* and 1*D*, $*P < .05$). On histologic examination of involved colon of 0.8% OXA-treated wild-type (WT) mice, we observed a superficial inflammation characterized by the presence of epithelial cell loss and patchy ulceration, pronounced depletion of mucin-producing goblet cells, and reduction of the density of the tubular glands. In addition, in the LP, a mixed inflammatory cell infiltrate consisting of lymphocytes and granulocytes was associated with an exudation of cells into the bowel lumen. These histopathologic changes of OXA-induced colitis were more serious in the colon of CD30LKO mice than in WT mice, and the histologic score of the colon was significantly higher in CD30LKO mice than in WT mice on day 2 after OXA administration (Figure 1*E* and *F*, $*P < .05$). Thus, CD30LKO mice were highly susceptible to OXA-induced colitis compared with control WT mice.

### *Cell Accumulation in the Colon Mucosa of CD30LKO Mice With OXA-Induced Colitis*

Populations of LP cells in the large intestines from CD30LKO mice before and on day 4 after 0.8% OXA administration were analyzed by flow cytometry. As shown in Supplemental Figure 2*A* (see Supplemental Figure 2*A* online at www.gastrojournal.org), the proportions of $CD11b^+Gr\text{-}1^+$ and $CD11b^+F4/80^+$ cells were significantly higher than OXA-treated WT mice ($*P < .05$), whereas the proportions of $\gamma\delta TCR^+CD3^+$ and $DX5^+CD3^-$ cells had slightly decreased in OXA-treated CD30LKO mice compared with OXA-treated WT mice (see Supplemental Figure 2*B* online at www.gastrojournal.org, $*P < .05$ or $**P < .01$). The relative numbers of $CD4^+CD25^+$ and $CD4^+CD44^+$ T cells were significantly lower in CD30LKO mice before or after OXA-administration (see Supplemental Figure 2*C* online at www.gastrojournal.org, $*P < .05$). Intracellular staining analysis for expression of Foxp3 revealed that $CD4^+CD25^+$ T cells were divided into 2 populations on the basis of Foxp3 expression.[35] $CD4^+CD25^+Foxp3^-$ T cells were selectively reduced in CD30LKO mice before and after OXA administration (see Supplemental Figure 2*D* online at www.gastrojournal.org, $*P < .05$). CD30L was expressed by $CD4^+CD25^+Foxp3^-$ T cells but not by $CD4^+CD25^+Foxp3^+$ T cells (see Supplemental Figure 2*D* online at www.gastrojournal.org).

### *Cytokine Production by LP Cells of CD30LKO Mice With OXA-Induced Colitis*

The spontaneous release levels of IFN-γ, TNF-α, IL-12p40, and IL-10 were significantly lower in CD30LKO mice than in WT mice before and on day 4 after 0.8% OXA administration (Figure 2*A*, $*P < .05$ or $**P < .01$), but the levels of IL-1β and IL-6 were significantly higher in CD30L KO mice than in WT mice ($*P < .05$ and $**P < .01$). The secretion of IL-4 and IL-13 were significantly higher, but the levels of IL-10 and IFN-γ were significantly lower in naïve and OXA-treated

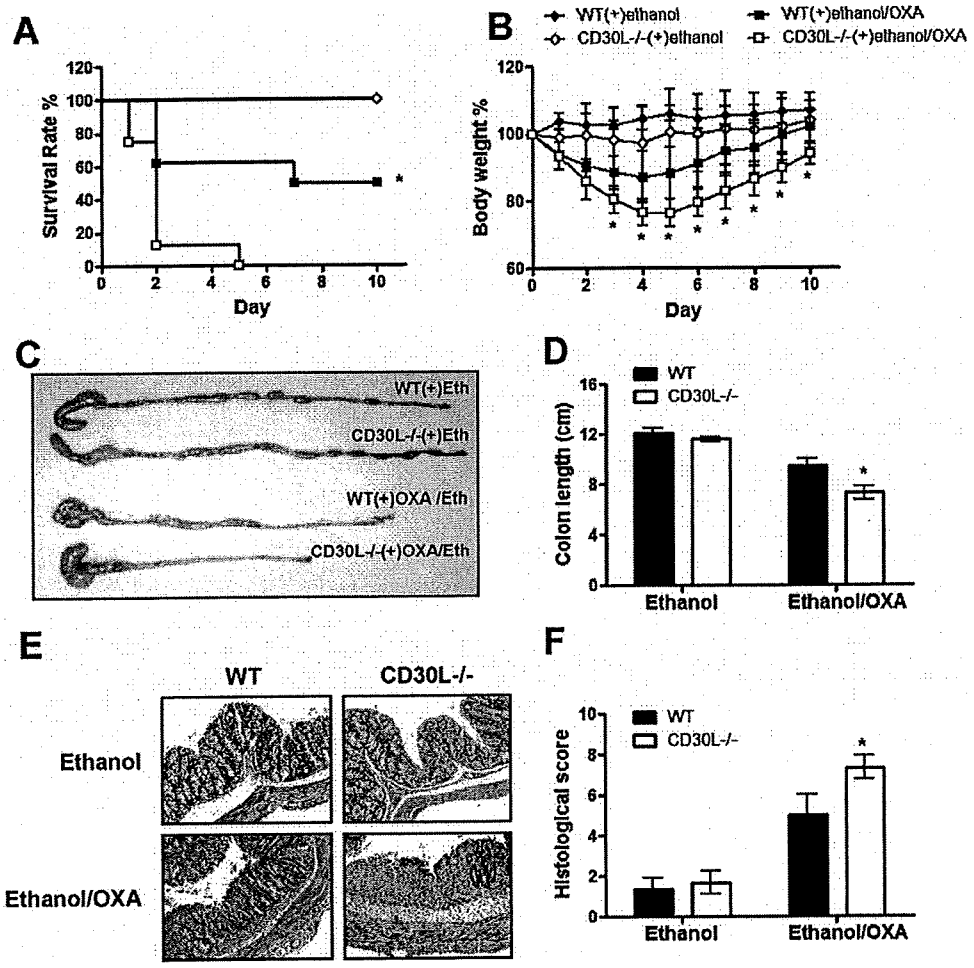


**Figure 1.** Susceptibility of CD30L$^{-/-}$ mice to OXA-induced colitis. Survival rate (*A*) and weight loss (*B*) of mice after intrarectal administration of 1% or 0.8% OXA, respectively. (*C*) Macroscopic changes of colons on day 2 after administration of 0.8% OXA. (*D*) Colon length measured on day 2 after 0.8% OXA administration. (*E*) Histologic analysis of the colons from mice on day 2 after 0.8% OXA administration (original magnification, ×200). (*F*) Histologic scores of the colons from ethanol- and OXA-treated WT and CD30L$^{-/-}$ mice. Data shown represent mean values ± SD of 24 mice of each group obtained from 3 independent experiments. Statistically significant differences from the value for OXA-treated WT mice are shown (*$P < .05$).

CD30LKO mice than WT mice upon stimulation with anti-CD3/anti-CD28 mAbs (Figure 2*B*, *$P < .05$ or **$P < .01$).

To identify T-cell populations producing IFN-γ, IL-4, or IL-10, we examined intracellular cytokine flow cytometry analysis on LP T cells in OXA-induced colitis. CD4$^+$ T cells were major producers of IL-4 and IL-10 (Figure 3*A* and 3*C*), whereas CD4$^-$ T cells produced an appreciable level of IFN-γ in addition to CD4$^+$ T cells (Figure 3*B*). The absolute numbers of IL-4$^+$CD4$^+$ T cells were significantly higher in naïve and OXA-treated CD30LKO mice than in WT mice (Figure 3*A*, *$P < .05$ or **$P < .01$). The absolute numbers of IFN-γ$^+$CD4$^+$ T cells and IL-10$^+$CD4$^+$ T cells were significantly lower in OXA-treated CD30LKO mice compared with OXA-treated WT mice (Figure 3*B* and *C*, **$P < .01$). We further characterized these CD4$^+$ T cells in the LP of the colon in mice with OXA-induced colitis. IFN-γ was produced mainly by the CD4$^+$CD25$^-$ T-cell population, whereas CD4$^+$CD25$^+$ T cells mainly produced IL-10. CD4$^+$CD30L$^-$ T cells preferentially produced IFN-γ and IL-10 (see Supplemental Figure 2*E* and *F* online at www.gastrojournal.org).

### *In Vivo Treatment With Anti-IL-4 mAb Ameliorates OXA-Induced Colitis in CD30LKO Mice*

To determine the involvement of elevated IL-4 in the pathogenesis of OXA-induced colitis in CD30LKO mice, we examined the effect of in vivo administration of anti-IL-4 mAb on OXA-induced colitis in CD30L KO mice. In vivo injection of more than 0.3 mg anti-IL-4 mAb significantly ameliorated OXA-induced colitis in CD30LKO mice (Figure 4*A–C*, *$P < .05$ or **$P < .01$). The levels of IL-10 and IFN-γ were significantly higher in anti-IL-4 mAb- and OXA-treated CD30LKO mice than in control IgG- and OXA-treated

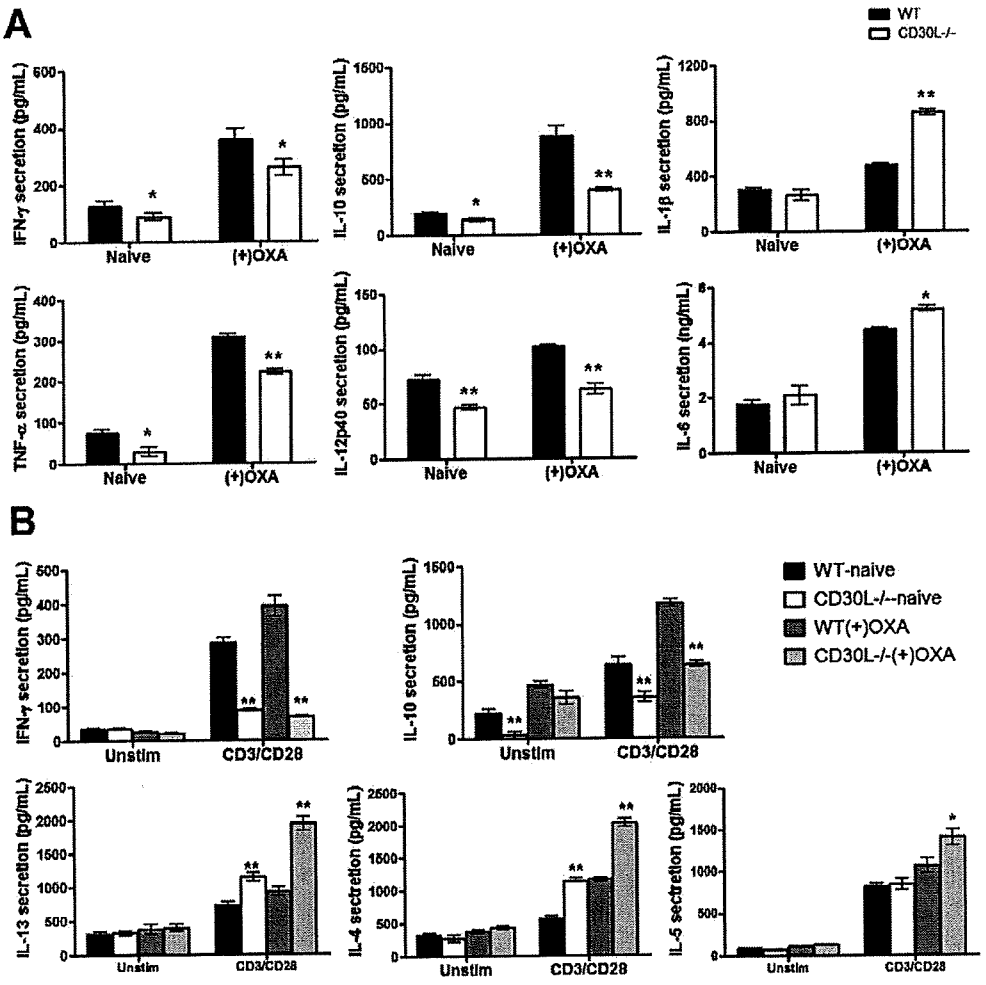


**Figure 2.** Cytokine production of LP cells in large intestines in OXA-inducted colitis after 24 hours cultured without any stimulation (*A*) and 48 hours cultured with anti-CD3/CD28 mAbs (*B*). Each *column* and *vertical bar* indicates means ± SD for 5 mice of each group. Data of a representative experiment are shown from 3 independent experiments. Statistically significant differences are shown (*$P < .05$ or **$P < .01$).

CD30LKO mice upon stimulation with anti-CD3/anti-CD28 mAbs, (Figure 4*D*, *$P < .05$ or **$P < .01$). IL-13 production was not affected in CD30LKO mice by anti-IL-4 mAb treatment. Similarly, anti-IL-4 mAb treatment ameliorated OXA-induced colitis in WT mice (see Supplemental Figure 3 online at www.gastrojournal.org). Thus, these results suggest that IL-4 is involved in the pathogenesis of OXA-induced colitis in WT and CD30LKO mice.

### *In Vivo Treatment With Agonistic Anti-CD30 mAb Ameliorates OXA-Induced Colitis in CD30LKO and WT Mice*

To elucidate the roles of CD30L/CD30 signaling in OXA-induced colitis, we examined the effect of in vivo administration of agonistic anti-CD30 mAb (CD30.1)[18] on OXA-induced colitis in CD30L KO mice. Mice were injected IP with anti-CD30 mAb or control hamster IgG1 24 hours before 1% OXA administration for survival rate or 0.8 % OXA treatment for weight loss. In vivo injection of anti-CD30 mAb significantly protected against OXA-induced colitis in CD30LKO mice as assessed by both survival rate and weight loss (Figure 5*A*, *$P < .05$ or **$P < .01$). These results suggest that CD30 signaling is important for controlling OXA-induced colitis. The secretion of IL-4 and IL-13 were significantly lower, but the levels of IL-10 and IFN-γ were significantly higher in anti-CD30 mAb- and OXA-treated CD30LKO mice than in control antibody and OXA-treated CD30LKO mice upon stimulation with anti-CD3/anti-CD28 mAbs (Figure 5*B*, *$P < .05$ or **$P < .01$). Thus, these results suggest that stimulating reagent for CD30 signaling may be useful to control OXA-induced colitis.

We further examined the effect of in vivo treatment with agonistic anti-CD30 mAb on OXA-induced colitis in WT mice. Although in vivo treatment with anti-CD30 mAb 1 day after 1.5% OXA administration did not affect

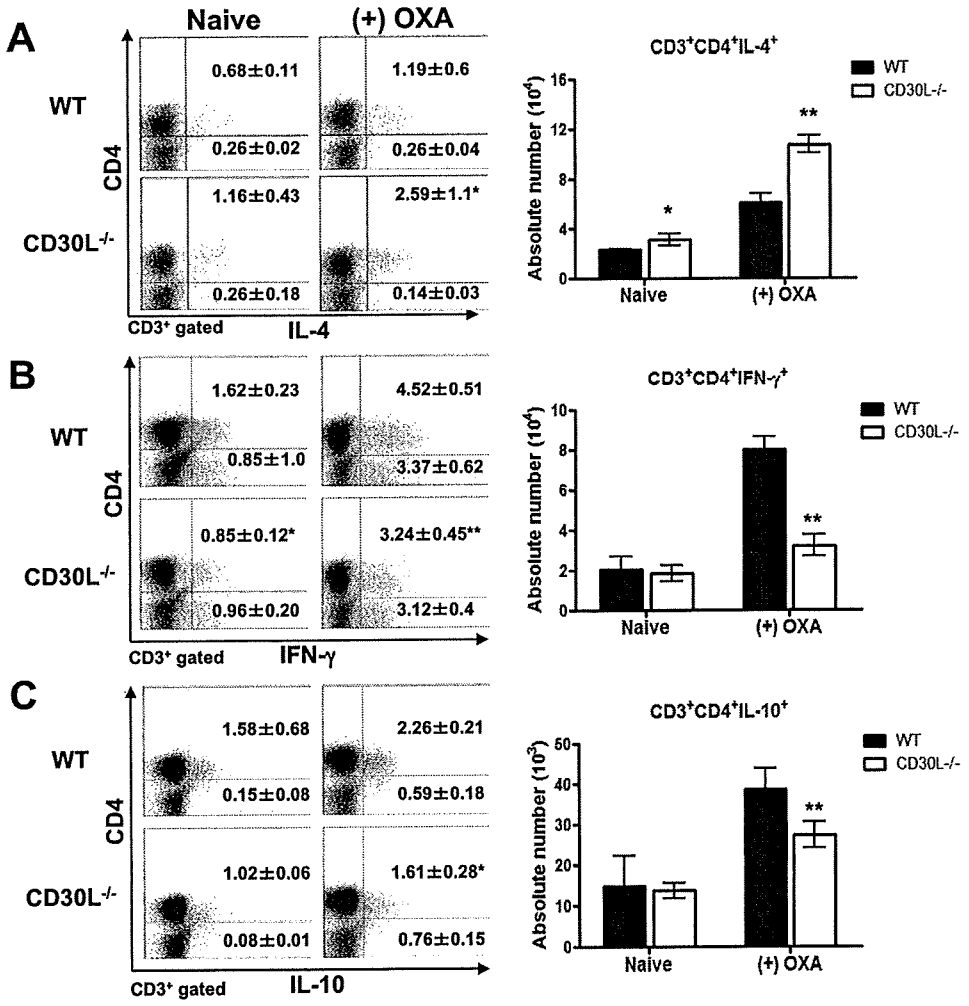


**Figure 3.** Intracellular cytokine expression by LP T cells from OXA-treated CD30L$^{-/-}$ mice. LP T cells from mice treated with 0.8% OXA 4 days previously were cultured with PMA plus ionomycin and analyzed for the expression of CD4 and IL-4 (*A*), IFN-γ (*B*), or IL-10 (*C*) by intracellular staining. The absolute number of each subset was calculated by multiplying the total number of LP T cells by the percentage of each subset. *Values* of each *column* and *vertical bar* indicate means ± SD for 5 mice within each group. Representative data are shown from 3 independent experiments. Statistically significant differences are shown (*$P < .05$ or **$P < .01$).

OXA-induced colitis, the treatment 1 day before or at the same time as OXA administration significantly extended the survival period and decreased weight loss of WT mice with OXA-induced colitis (Figure 5*C*, **$P < .01$). Thus, anti-CD30 mAb may be useful as a novel biologic therapy for UC.

### *CD30LKO Mice Are Resistant to TNBS-Induced Acute Colitis*

TNBS-induced acute colitis is thought to be a Th1 cell-mediated inflammation.[11–13] To examine the role of CD30L in development of TNBS-induced acute colitis in mice, we next examined TNBS-induced acute colitis with a Th1-like response in CD30LKO mice with C57BL/6 background. The CD30L was expressed mainly on a part of CD4$^+$ T cells from freshly isolated LPL in naïve C57BL/6 mice and mice treated with TNBS 7 days previously (see Supplemental Figure 1*A* online at www.gastrojournal.org). The CD30 expression on CD4$^+$ T cells from LPL was detected only when the LPLs were cultured in vitro and the level of CD30$^+$ in CD4$^+$ cells were significantly increased in mice with TNBS-induced colitis than naive mice (see Supplemental Figure 1*C* online at www.gastrojournal.org, *$P < .05$).

As shown in Figure 6*A* and *B*, TNBS-induced acute colitis was attenuated in CD30LKO mice as indicated by survival rate and weight loss (*$P < .05$). Macroscopic inspection showed a significantly longer colon in CD30LKO mice than in WT mice on day 7 after TNBS administration (Figure 6*C*, *$P < .05$). The histologic score of the colon was significantly lower in CD30LKO mice than in WT mice (Figure 6*D*, **$P < .01$).

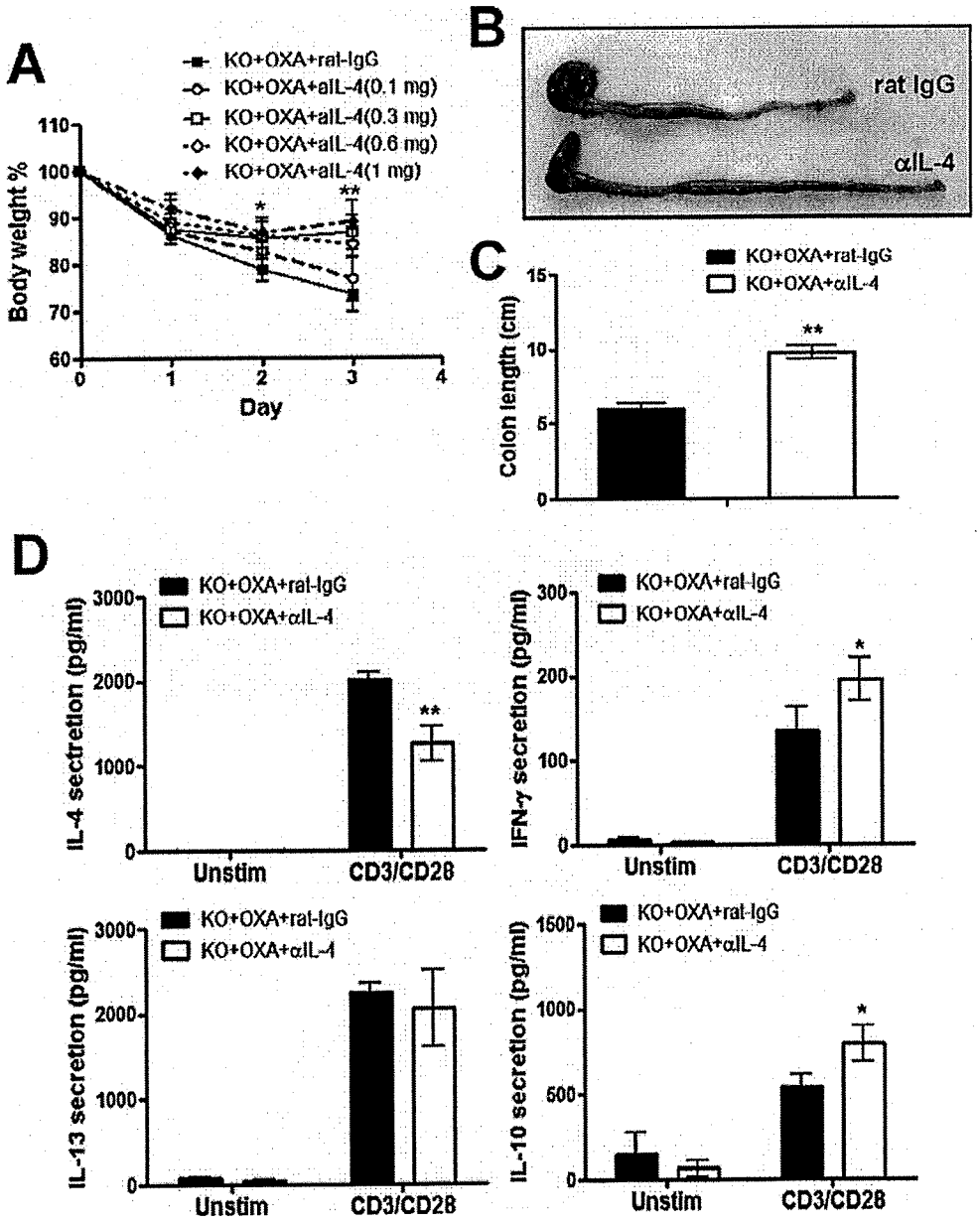


**Figure 4.** Effects of in vivo treatment with anti-IL-4 mAb on OXA-induced colitis. CD30L$^{-/-}$ mice were treated with indicated doses of anti-IL-4 or control rat IgG at the time of colitis induction with OXA. The body weight (*A*) and macroscopic appearance of colons (*B*), colon length (*C*), or cytokine production (*D*) on day 3 after OXA and 0.3 mg of anti-IL-4 mAb administration. Each *column* and *vertical bar* indicates means ± SD for 5 mice of each group. Data of a representative experiment are shown from 3 independent experiments. Statistically significant differences are shown (*$P < .05$ or **$P < .01$).

To determine whether CD30 signaling is involved in TNBS-induced acute colitis, we examined the effect of in vivo administration of agonistic anti-CD30 mAb to CD30LKO mice with TNBS-induced colitis. Anti-CD30 mAb aggravated TNBS-induced colitis in CD30LKO mice as assessed by both survival rate and body weight (Figure 6*E*, *$P < .05$ or **$P < .01$). Thus, these results indicate that CD30L/CD30 signaling is involved in development of TNBS-induced acute colitis.

### *Cytokine Production by LP Cells of CD30LKO Mice With TNBS-Induced Acute Colitis*

The levels of IFN-γ, TNF-α, IL-1β, IL-6, and IL-12p40 production by LP cells without stimulation were significantly lower but IL-10 secretion was higher in CD30LKO mice than in WT mice on day 7 after TNBS administration (Figure 7*A*, * $P < .05$ or **$P < .01$). The secretion of IL-4, IL-13, and IL-10 was significantly higher

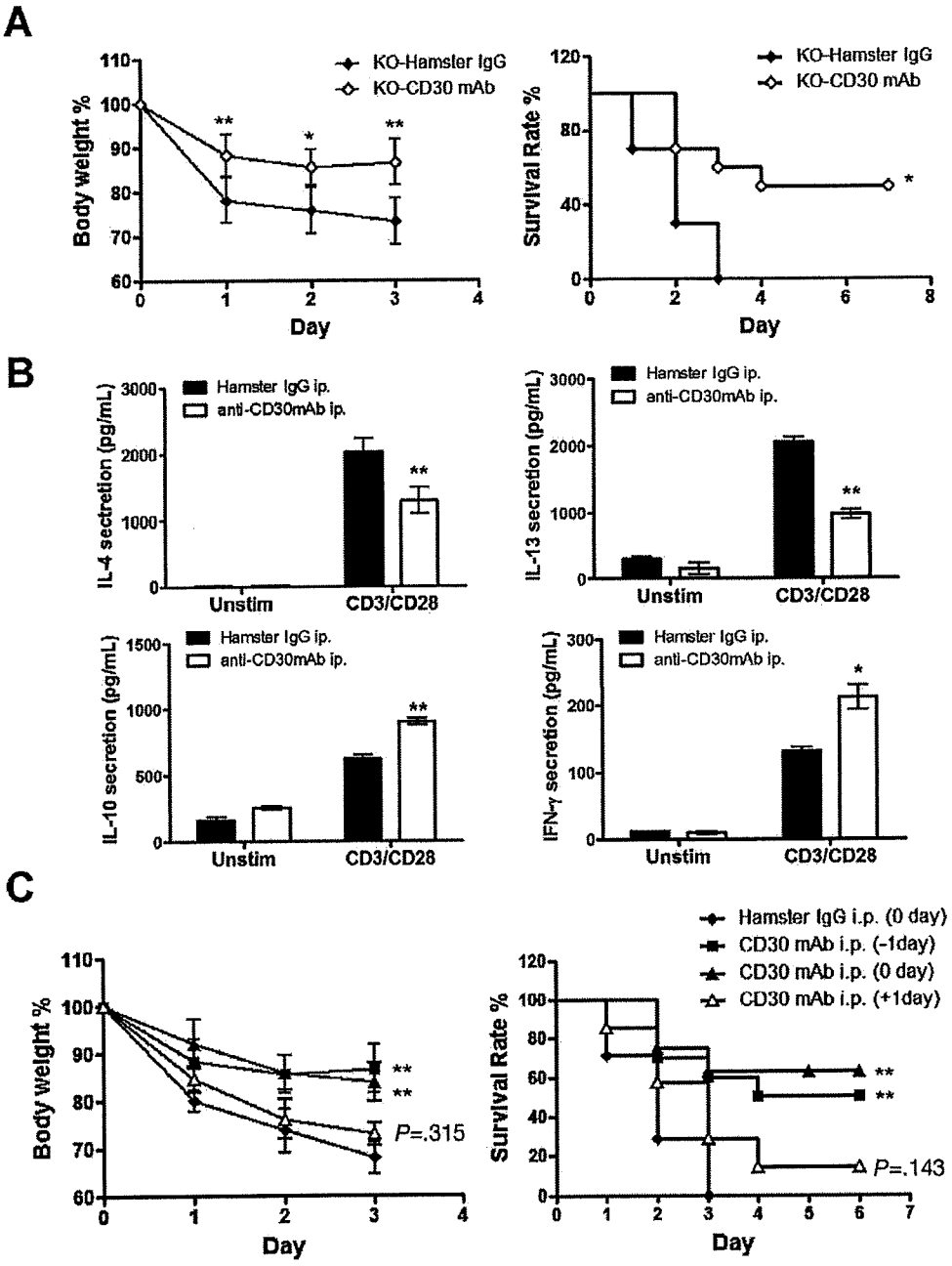


**Figure 5.** Effects of in vivo treatment with agonistic anti-CD30 mAb on OXA-induced colitis. (*A*) Anti-CD30 mAb (100 μg/head, clone CD30.1) or hamster IgG1 was injected intraperitoneally into CD30L$^{-/-}$ mice on day 1 before 1% OXA administration, and then weight loss and survival rates were monitored daily. (*B*) LP T cells of anti-CD30 mAb and 0.8% OXA-treated CD30L$^{-/-}$ mice were cultured coating with or without anti-CD3/CD28 mAbs, and cytokines secretion were assayed by ELISA on day 4 after OXA treated. (*C*) Anti-CD30 mAb or hamster IgG1 was injected intraperitoneally into WT mice on day −1, day 0, or day 1 after 1.5% OXA treated, and weight loss and survival rates were monitored daily. Each *column* and *vertical bar* indicates means ± SD for 6–10 mice of each group obtained from a representative experiment in 3 independent experiments. Statistically significant differences from control hamster IgG1- and OXA-treated mice are shown (*$P < .05$ or **$P < .01$).

but the level of IFN-γ was significantly lower in TNBS-treated CD30LKO mice than in TNBS-treated WT mice upon stimulation with anti-CD3/CD28 mAbs (Figure 7*B*, *$P < .05$ or $P < .01$). These results suggest that CD30L signaling is involved in development of TNBS-induced acute colitis in association with Th1-like response.

## Discussion

In the present study, we found that OXA-induced colitis was exacerbated in CD30LKO mice, of which CD4$^+$ T cells in the LP of large intestine produced higher levels of Th2-type cytokines but less IFN-γ than those in

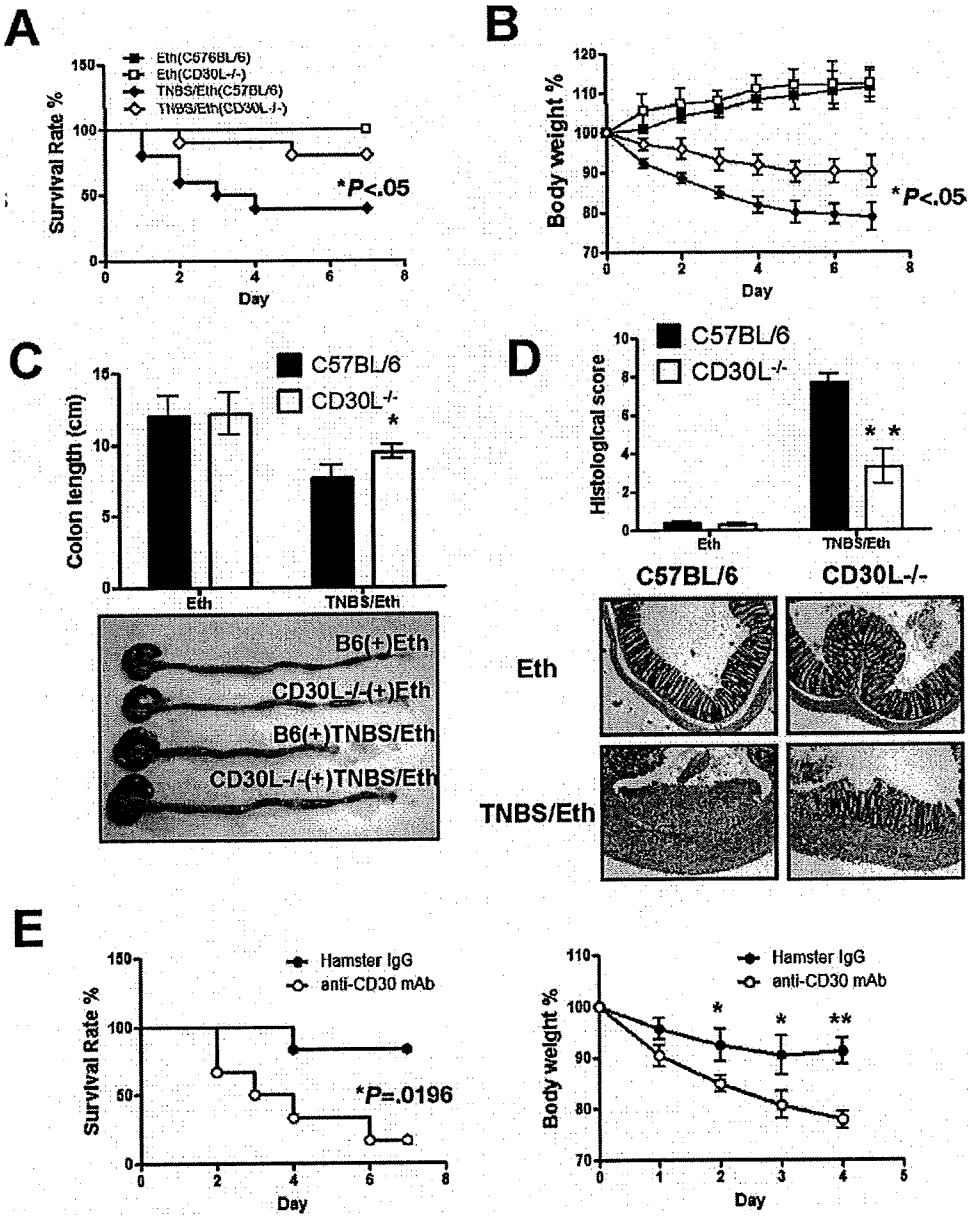


**Figure 6.** Susceptibility of CD30L$^{-/-}$mice to TNBS-induced acute colitis. CD30L$^{-/-}$ mice were administered 3 mg TNBS/mouse, and, thereafter, survival rate (*A*) and body weight (*B*) were monitored every day. (*C*) Macroscopic changes of colons and colon length and (*D*) histologic analysis and score were analyzed on day 7 after TNBS treatment. (*E*) In vivo administered with anti-CD30 mAb to CD30L$^{-/-}$ mice with TNBS induced colitis, and then survival rate and body weight were monitored every day. Data shown represent mean values ± SD of 10 mice of each group obtained from 3 independent experiments. Statistically significant differences are shown (*$P < .05$ or **$P < .01$).

WT mice. However, CD30LKO mice are resistant to TNBS-induced colitis with impaired IFN-γ production in LP T cells of the colon. Thus, Th1-like immunity characterized by IFN-γ production was impaired, whereas Th2-like immunity capable of producing IL-4 and IL-13 was enhanced in both murine experimentally induced colitis models in CD30LKO mice. Stimulation with CD30 signaling by agonistic anti-CD30 mAb increased Th1-like response in the mucosa of colons and ameliorated the course of OXA-induced colitis but aggravated TNBS-induced acute colitis in CD30LKO mice. These results proved that CD30 signaling via CD30L played a role in controlling colitis by deviating the balance of Th1/Th2 to Th1 response in colon.

Th1 cells inhibit the proliferation of Th2 cells, and Th2 cells shut down IFN-γ production by Th1 cells, indicating that Th1 and Th2 cells are mutually regulated.[36,37] Therefore, it is most likely that the Th1 response producing IFN-γ is selectively suppressed in the mucosa of the colon of CD30LKO mice, resulting in the dominant

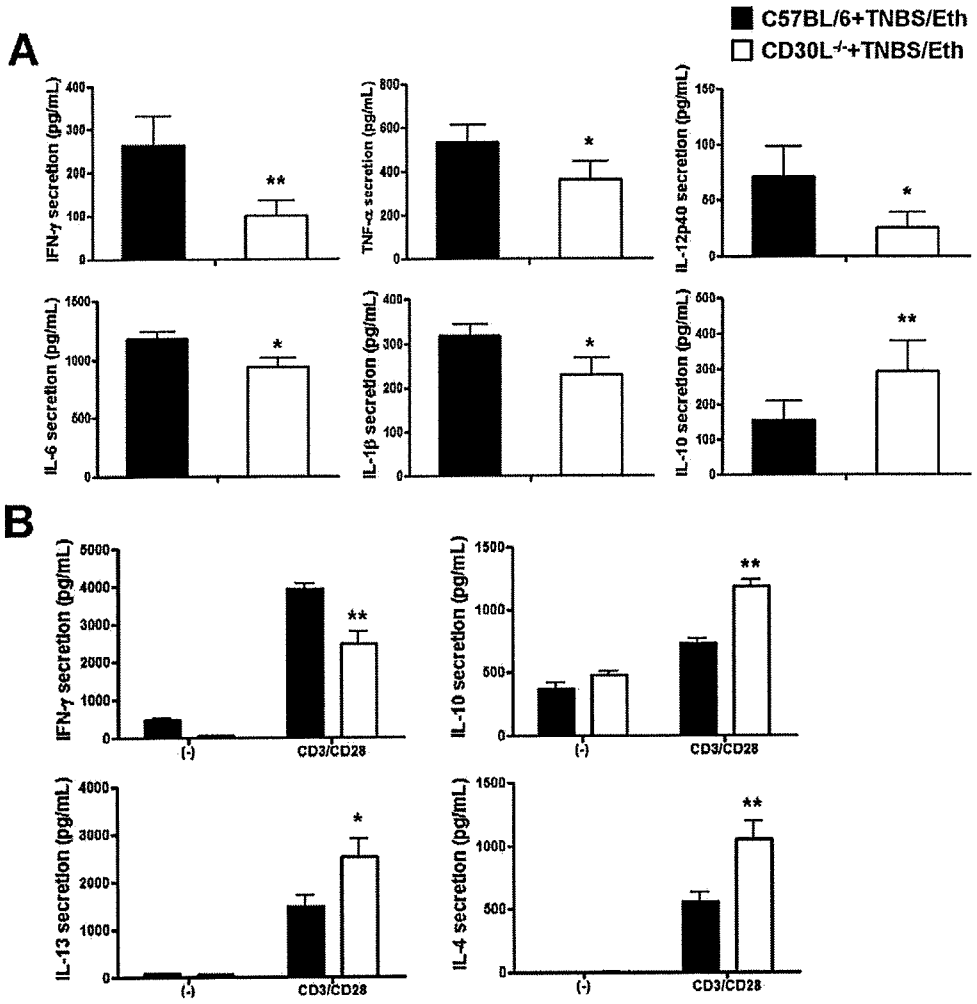


**Figure 7.** Cytokine production of LP cells in TNBS-induced colitis and effects of in vivo treatment with agonistic anti-CD30 mAb on TNBS-induced colitis in CD30LKO mice. (*A*) Cytokine production of LP cells in TNBS-induced colitis after culture without any stimulation. (*B*) Cytokine production of LP T cells in TNBS-induced colitis after culture with anti-CD3/CD28 mAbs. Culture supernatants were analyzed for concentrations of cytokines by specific ELISA. Each *column* and *vertical bar* indicates means ± SD for 5 mice of each group. Data of a representative experiment are shown from 3 independent experiments. Statistically significant differences are shown (*$P < .05$ or **$P < .01$).

Th2 responses. As a consequence, OXA-induced colitis was exaggerated but TNBS-induced colitis was ameliorated in CD30LKO mice. CD30L is expressed on activated T cells irrespective of Th1 and Th2 types, macrophages, DC, and B cells.[19–22] On the other hand, CD30 has been reported to be preferentially expressed by effector and memory Th cells but not by macrophage/DC or B cells.[23–26] We showed here that CD30L was expressed mainly by a part of freshly isolated $CD4^+$ T cells but not apparently by B cells or DC/macrophages in the colon of naïve mice. Although CD30 expression was not detected on freshly isolated $CD4^+$ T cells in the colon of naive mice and mice with colitis, it was apparent after in vitro culture with or without anti-CD3 mAb stimulation. It is notable that the numbers of $CD30^+$ T cells in $CD4^+$ population of the colon were significantly increased after induction of colitis by OXA or TNBS. These results suggest that CD30/CD30L signaling executed by $CD30^+$ T cell to $CD30L^+$ T cell interaction may at least partly responsible for Th responses in the colon.

It has recently been reported that both UC in humans and OXA-induced colitis in mice are at least partly mediated by CD1d-restricted NKT cells producing IL-13.[17,38] Furthermore, both Th1 and Th2 pathways have been implicated in the pathogenesis of OXA-induced colitis.[39] We found in our study no difference in the number of $DX5^+CD3^+$ T cells in the LP of the colon between CD30LKO and WT mice. The experiment with anti-IL-4 mAb treatment revealed the involvement of IL-4 in OXA-colitis in CD30LKO and WT mice. CD30L/CD30 signaling may be involved in the shift of $CD4^+$ Th1/Th2 balance to Th1 type. Blazar et al have recently reported that the homing of alloreactive $CD4^+$ T cells to the gastrointestinal tract was inhibited in CD30LKO recipi-

ents, leading to reduced mortality and lower weight loss in graft vs host disease.[40] CD30L/CD30 signaling is reported to be involved in chemokine receptor expression.[32,41] Therefore, it is also possible that migration of $CD4^+$ Th1 cells to the colon may be selectively impaired in CD30LKO mice. Further experiments are required to elucidate these possibilities.

It is noted that IL-10 production by $CD4^+CD25^+Foxp3^-$ T cells corresponding to T-regulatory type1 (Tr1) cells were fewer in the LP of CD30LKO mice. T cells capable of producing IL-10 in the intestine are termed *Tr1 cells*, which are able to prevent the development of experimentally induced colitis when transferred in vivo.[42–44] Therefore, it is also speculated that CD30L/CD30 signaling plays a role in induction of Tr1 cells producing IL-10, which may contribute to attenuate the development of colitis. However, IL-10 production was impaired in CD30LKO mice with OXA-induced colitis, whereas it was augmented in CD30LKO mice with TNBS-induced colitis. Considering all of the data, it appears that CD30L plays a critical role in deviating $CD30^+$ Th cells to Th1 cells in the colon, which may regulate the development of both OXA-induced and TNBS-induced acute colitis.

It is notable in our study that therapeutic application of the agonistic anti-CD30 mAb ameliorated OXA-induced colitis in WT mice. Furthermore, attenuation of colitis induced by TNBS in CD30LKO mice suggests that neutralizing anti-CD30 mAb is potentially useful for control of TNBS-induced colitis. Taken together, our study suggests that Abs against CD30L/CD30 could be a novel biologic therapy for IBD.

## Supplementary Data

Note: To access the supplementary material accompanying this article, visit the online version of *Gastroenterology* at www.gastrojournal.org, and at doi:10.1053/j.gastro.2007.11.004.

### References


1. Macdonald TT, Monteleone G. Immunity, inflammation, and allergy in the gut. Science 2005;307:1920–1925.
2. Fiocchi C. Inflammatory bowel disease: etiology and pathogenesis. Gastroenterology 1998;115:182–205.
3. Sartor RB. The influence of normal microbial flora on the development of chronic mucosal inflammation. Res Immunol 1997; 148:567–576.
4. Maaser C, Kagnoff MF. Role of the intestinal epithelium in orchestrating innate and adaptive mucosal immunity. Gastroenterology 2002;40:525–529.
5. Bouma G, Strober W. The immunological and genetic basis of inflammatory bowel disease. Nat Rev Immunol 2003;3:521–533.
6. Targan SR, Karp LC. Defects in mucosal immunity leading to ulcerative colitis. Immunol Rev 2005;206:296–305.
7. Cobrin GM, Abreu MT. Defects in mucosal immunity leading to Crohn's disease. Immunol Rev 2005;206:277–295.
8. Kuhn R, Lohler J, Rennick D, et al. Interleukin-10-deficient mice develop chronic enterocolitis. Cell 1993;75:263–274.
9. Powrie F, Leach MW, Mauze S, et al. Inhibition of Th1 responses prevents inflammatory bowel disease in scid mice reconstituted with $CD45RB^{hi}$ $CD4^+$ T cells. Immunity 1994;1:553–562.
10. Morris GP, Beck PL, Herridge MS, et al. Hapten-induced model of chronic inflammation and ulceration in the rat colon. Gastroenterology 1989;96:795–803.
11. Neurath MF, Fuss I, Kelsall BL, et al. antibodies to interleukin 12 abrogate established experimental colitis in mice. J Exp Med 1995;182:1281–1290.
12. Fuss IJ, Marth T, Neurath MF, et al. Anti-interleukin 12 treatment regulates apoptosis of Th1 T cells in experimental colitis in mice. Gastroenterology 1999;117:1078–1088.
13. Fichtner-Feigl S, Fuss IJ, Preiss JC, et al. Treatment of murine Th1- and Th2-mediated inflammatory bowel disease with NF-κB decoy oligonucleotides. J Clin Invest 2005;115:3057–3071.
14. Sadlack B, Merz H, Schorle H, et al. Ulcerative colitis-like disease in mice with a disrupted interleukin-2 gene. Cell 1993;75:253–261.
15. Mombaerts P, Mizoguchi E, Grusby MJ, et al. Spontaneous development of inflammatory bowel disease in T-cell receptor mutant mice. Cell 1993;75:275–282.
16. Boirivant M, Fuss IJ, Chu A, et al. Oxazalone colitis: a murine model of T helper cell type 2 colitis treatable with antibodies to interleukin 4. J Exp Med 1998;188:129–139.
17. Heller F, Fuss IJ, Nieuwenhuis EE, et al. Oxazolone colitis, a Th2 colitis model resembling ulcerative colitis, is mediated by IL-13-producing NK-T cells. Immunity 2002;17:629–638.
18. Croft M. Co-stimulatory members of the TNFR family: keys to effective T-cell immunity? Nat Rev Immunol 2003;3:609–620.
19. Kennedy MK, Willis CR, Armitage RJ. Deciphering CD30 ligand biology and its role in humoral immunity. Immunology 2006;118: 143–152.
20. Shimozato O, Takeda K, Yagita H, et al. Expression of CD30 ligand (CD153) on murine activated T cells. Biochem Biophys Res Commun 1999;256:519–526.
21. Cerutti A, Schaffer A, Goodwin RG, et al. Engagement of CD153 (CD30 ligand) by $CD30^+$ T cells inhibits class switch DNA recombination and antibody production in human $IgD^+$ $IgM^+$ B cells. J Immunol 2000;165:786–794.
22. Kim MY, Gaspal FM, Wiggett HE, et al. $CD4^+CD3^-$ accessory cells costimulate primed CD4 T cells through OX40 and CD30 at sites where T cells collaborate with B cells. Immunity 2003;8: 643–653.
23. Ellis TM, Simms PE, Slivnick DJ, et al. CD30 is a signal-transducing molecule that defines a subset of human activated $CD45RO^+$ T cells. J Immunol 1993;151:2380–2389.
24. Bowen MA, Lee RK, Miragliotta G, et al. Structure and expression of murine CD30 and its role in cytokine production. J Immunol 1996;156:442–449.
25. Smith CA, Gruss HJ, Davis T, et al. CD30 antigen, a marker for Hodgkin's lymphoma, is a receptor whose ligand defines an emerging family of cytokines with homology to TNF. Cell 1993; 73:1349–1360.
26. Romagnani S, Del Prete G, Maggi E, et al. CD30 and type 2 T helper (Th2) responses. J Leukoc Biol 1995;57:726–530.
27. Munk ME, Kern P, Kaufmann SH. Human $CD30^+$ cells are induced by *Mycobacterium tuberculosis* and present in tuberculosis lesions. Int Immunol 1997;9:713–720.
28. Flórido M, Borges M, Yagita H, et al. Contribution of CD30/CD153 but not of CD27/CD70, CD134/OX40L, or CD137/$4^-$1BBL to the optimal induction of protective immunity to *Mycobacterium avium*. J Leukoc Biol 2004;76:1039–1046.
29. Gerli R, Lunardi C, Vinante F, et al. Role of $CD30^+$ T cells in rheumatoid arthritis: a counter-regulatory paradigm for Th1-driven diseases. Trends Immunol 2001;22:72–77.

30. Saraiva M, Smith P, Fallon PG, et al. Inhibition of type 1 cytokine-mediated inflammation by a soluble CD30 homologue encoded by ectromelia (mousepox) virus. J Exp Med 2002;196:829–839.
31. Giacomelli R, Passacantando A, Parzanese I, et al. Serum levels of soluble CD30 are increased in ulcerative colitis (UC) but not in Crohn's-disease (CD). Clin Exp Immunol 1998;111:532–535.
32. Podack ER, Strbo N, Sotosec V, et al. CD30–Governor of memory T cells? Ann N Y Acad Sci 2002;975:101–113.
33. Nishimura H, Yajima T, Muta H, et al. A novel role of CD30/CD30L signaling in the generation of long-lived memory $CD8^+$T cells. J Immunol 2005;175:4627–4634.
34. Yoshihara K, Yajima T, Kubo C, et al. The role of IL-15 in colitis induced by dextran sulphate sodium in mice. Gut 2006;55:334–341.
35. Vieira PL, Christensen JR, Minaee S, et al. IL-10-secreting regulatory T cells do not express Foxp3 but have comparable regulatory function to naturally occurring $CD4^+CD25^+$ regulatory T cells. J Immunol 2004;172:5986–5993.
36. Murphy KM, Reiner SL. The lineage decisions of helper T cells. Nat Rev Immunol 2002;2:933–944.
37. Ansel KM, Djuretic I, Tanasa B, et al. Regulation of Th2 differentiation and IL-4 locus accessibility. Annu Rev Immunol 2006;24:607–656.
38. Fuss IJ, Heller F, Boirivant M, et al. Nonclassical CD1d-restricted NK T cells that produce IL-13 characterize an atypical Th2 response in ulcerative colitis. J Clin Invest 2004;113:1490–1497.
39. Iijima H, Neurath MF, Nagaishi T, et al. Specific regulation of T helper cell 1-mediated murine colitis by CEACAM1. J Exp Med 2004;199:471–482.
40. Blazar BR, Levy RB, Mak TW, et al. CD30/CD30 ligand (CD153) interaction regulates $CD4^+$ T cell-mediated graft-versus-host disease. J Immunol 2004;173:2933–2941.
41. Muta H, Boise LH, Fang L, et al. CD30 signals integrate expression of cytotoxic effector molecules, lymphocyte trafficking signals, and signals for proliferation and apoptosis. J Immunol 2000;165:5105–5111.
42. Asseman C, Mauze S, Leach MW, et al. An essential role for interleukin 10 in the function of regulatory T cells that inhibit intestinal inflammation. J Exp Med 1999;190:995–1004.
43. Groux H, O'Garra A, Bigler M, et al. A $CD4^+$ T-cell subset inhibits antigen-specific T-cell responses and prevents colitis. Nature 1997;389:737–742.
44. Kemper C, Chan AC, Green JM, et al. Activation of human $CD4^+$ cells with CD3 and CD46 induces a T-regulatory cell 1 phenotype. Nature 2003;421:388–392.

**Received April 29, 2007. Accepted October 25, 2007.**

**Address requests for reprints to: Yasunobu Yoshikai, MD, PhD, Division of Host Defense, Center for Prevention of Infectious Disease, Medical Institute of Bioregulation, Kyushu University, Fukuoka 812-8582, Japan. e-mail: yoshikai@bioreg.kyushu-u.ac.jp; fax: (81) 92-642-6973.**

**Conflicts of interest: There are no conflicts of interest to disclose.**

**Supported, in part, by the Program of Founding Research Centers for Emerging and Reemerging Infectious Diseases (launched as a project commissioned by the Ministry of Education, Culture, Sports, Science and Technology [MEXT], Japan); a Grant-in-Aid for Scientific Research on Priority Areas, Japan Society for the Promotion of Science; and by grants from the Japanese Ministry of Education, Science and Culture (to Y.Y.).**

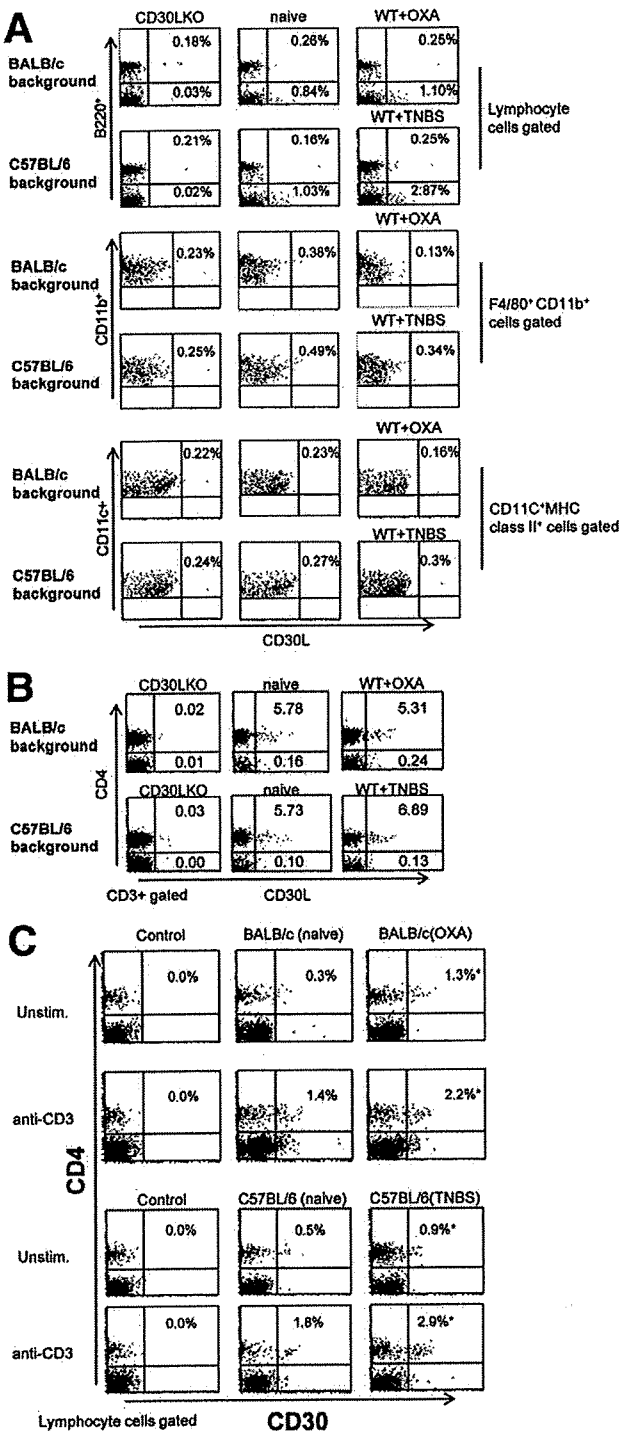


**Supplementary Figure 1.** Flow cytometry analysis of CD30L or CD30 expression on LP cells in the colon from naive and mice with colitis. (*A*) CD30L expression on laminal propria (LP) cells in the large intestine from naive CD30LKO mice (negative control) and naive WT mice or mice with colitis. Representative staining of various cell surface molecules on LP cells in the colon from mice before and on day 4 after OXA-administration or day 7 after TNBS-treatment. The results are presented as typical profiles after an analysis gate had been set on lymphocyte cells. F4/80$^+$CD11b$^+$ and CD11c$^+$MHC class II$^+$, (*B*) CD3$^+$. (*C*) LP cells of BALB/c or C57BL/6 mice before and after induction of colitis by 0.8% OXA or 3 mg TNBS were obtained and cultured in 96-well plate stimulation with or without 10 $\mu$g/mL anti-CD3 mAb. These cells were collected after 24 hr cultured and then analyzed by flow cytometry for CD30 expression with PE-CD30 and isotype control hamster IgG1. Values of each column and *vertical bar* indicate means ± SD for 5 mice within each group. Representative data are shown from 3 independent experiments. Statistically significant differences are shown (*$P < .05$).

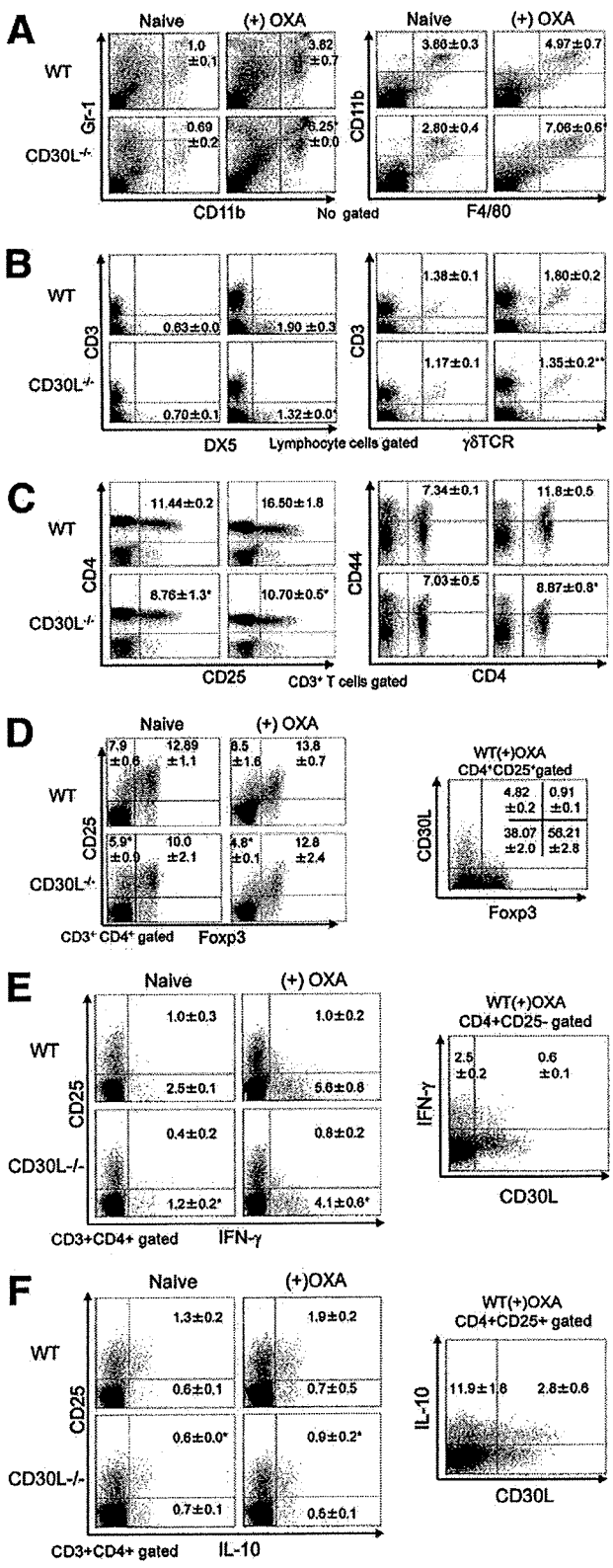


**Supplementary Figure 2.** Flow cytometry analysis of LP cells in the large intestine from naive and OXA-treated CD30L$^{-/-}$ mice. Representative staining of various cell surface molecules on LP cells in the colon from mice before and on day 4 after 0.8% OXA administration. The results are presented as typical profiles after an analysis gate had been set on no gate (*A*), lymphocytes (*B*), CD3$^+$ cells (*C*), CD3$^+$CD4$^+$ cells (*D*) and CD4$^+$CD25$^+$ cells. Intracellular cytokine expression by LP T cells from OXA-treated WT mice or CD30L$^{-/-}$ mice. LP T cells from naive or mice treated with 0.8% OXA 4 days previously were cultured with PMA plus ionomycin and analyzed for the expression of CD4, CD25, CD30L, and IFN-γ (*E*) or IL-10 (*F*) by intracellular staining. The absolute number of each subset was calculated by multiplying the total number of LP T cells by the percentage of each subset. Values of each *column* and *vertical bar* indicate means ± SD for 5 mice within each group. Representative data are shown from 3 independent experiments. Statistically significant differences are shown (*$P < .05$ or **$P < .01$).

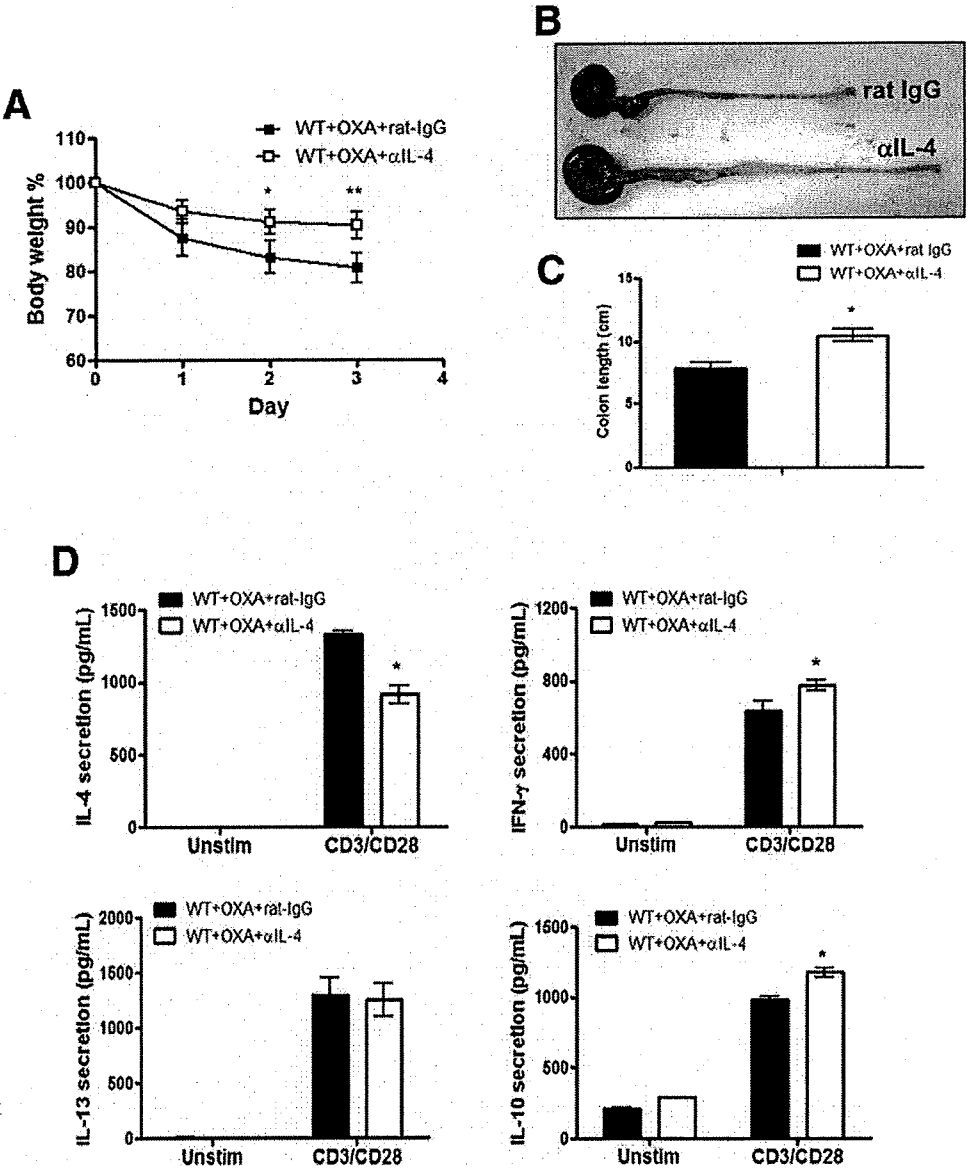


**Supplementary Figure 3.** Effects of in vivo treatment with anti-IL-4 mAb on OXA-induced colitis. WT mice were treated with anti-IL-4 (0.3 mg per dose) or control rat IgG (0.3 mg per dose) at the time of colitis induction with OXA. The body weight loss (*A*), macroscopic appearance of colons (*B*) and colon length (*C*) were monitored daily. Cytokine production (*D*) on day 3 after OXA treated was assayed by ELISA. Each *column* and *vertical bar* indicates means ± SD for 5 mice of each group. Data of a representative are shown from 3 independent experiments. Statistically significant differences are shown (*$P < .05$ or **$P < .01$).

*J. Biochem.* 143, 237–242 (2008)
doi:10.1093/jb/mvm212

# The Effects of Mutations in the Carboxyl-Terminal Region on the Catalytic Activity of *Escherichia coli* Signal Peptidase I

**Yong-Tae Kim[1,2], Hisashi Yoshida[1], Masaki Kojima[3], Ryo Kurita[1], Wataru Nishii[2,3], Tomonari Muramatsu[2], Hisashi Ito[1], Sun Joo Park[4,*] and Kenji Takahashi[3,†]**

*[1]Department of Chemistry, Faculty of Science and Engineering, Aoyama Gakuin University, Sagamihara, Kanagawa 229-8558; [2]RIKEN Genomic Sciences Center, Tsurumi, Yokohama 230-0045; [3]School of Life Sciences, Tokyo University of Pharmacy and Life Sciences, Hachioji, Tokyo 192-0392; and [4]Department of Biochemistry, Institute of Medical Science, University of Tokyo, Minato-ku, Tokyo 108-8539, Japan*

Received October 20, 2007; accepted October 30, 2007; published online November 21, 2007

***Escherichia coli* signal peptidase I (SPase I) is a membrane-bound serine endopeptidase that catalyses the cleavage of signal peptides from the pre-forms of membrane or secretory proteins. Our previous studies using chemical modification and site-directed mutagenesis suggested that $Trp^{300}$ and $Arg^{77}$, $Arg^{222}$, $Arg^{315}$ and $Arg^{318}$ are important for the proper and stable conformation of the active site of SPase I. Interestingly, many of these residues reside in the C-terminal region of the enzyme. As a continuation of these studies, we investigated in the present study the effects of mutations in the C-terminal region including amino acid residues at positions from 319 to 323 by deletions and site-directed mutagenesis. As a result, the deletion of the C-terminal $His^{323}$ was shown to scarcely affect the enzyme activity of SPase I, whereas the deletion of $Gly^{321}$-$His^{323}$ or $Ile^{319}$-$His^{323}$ as well as the point mutation of $Ile^{322}$ to alanine was shown to decrease significantly both the activity *in vitro* and *in vivo* without a big gross conformational change in the enzyme. These results suggest a significant contribution of $Ile^{322}$ to the construction and maintenance of the proper and critical local conformation backing up the active site of SPase I.**

**Key words: carboxyl-terminal residues, deletion, *Escherichia coli*, signal peptidase I, site-directed mutagenesis.**

Most membrane and secretory proteins in *Escherichia coli* are synthesized *in vivo* as precursors that bear an $NH_2$-terminal signal (leader) peptide of 15–30 amino acid residues. This signal sequence is involved in guiding the protein into the targeting and translocating pathway by interacting with the membrane and other components of the cellular secretory machinery. The signal peptides are removed by the action of signal peptidase I (leader peptidase, SPase I) during or shortly after the protein export (*1–3*). Following the discovery of *E. coli* SPase I (*4*), the enzyme was cloned (*5*), sequenced (*2*), overexpressed (*6*, *7*), purified (*2*, *7*, *8*, *9*) and enzymatically characterized (*7*, *10*) from a wild-type strain of *E. coli*. The substrate specificity has also been investigated, indicating that small, uncharged amino acids are usually present in the substrates at the –1 and –3 positions from the site of cleavage by SPase I (*11*). This enzyme is an integral membrane endopeptidase that is typically anchored to the membrane by amino-terminal transmembrane segments (*12*, *13*). The active site and the substrate recognition site of the enzyme are in the carboxyl-terminal domain that resides on the outer surface of the cytoplasmic membrane (*2*, *14*). Further, a soluble catalytically active SPase I (Δ2–75 SPase I), which lacks the two amino-terminal transmembrane segments (residues 1–22 and 62–75) and the cytoplasmic domain (residues 23–61), was produced (*15*) and crystallized (*16*, *17*). By using site-directed mutangenesis and chemical modification methods (*10*, *18–20*), the catalytic activity of SPase I was shown to depend on the operation of a serine-lysine catalytic dyad, whereby $Ser^{90}$ serves as the nucleophile and $Lys^{145}$ serves as the general base in the catalytic mechanism. The Ser–Lys catalytic dyad structure of SPase I has been recently confirmed by elucidation of the three-dimensional structure of the enzyme in complex with a β-lactam inhibitor (*3*, *16*). Results of the enzymatic characterization, site-directed mutagenesis, chemical modification and three-dimensional structure study indicated that *E. coli* SPase I belongs to a novel class of serine protenases (*7*, *18–23*) that utilize a Ser–Lys catalytic dyad mechanism as opposed to the more common Ser–His–Asp catalytic triad mechanism in the cleavage reaction (*3*).

In our previous studies, we investigated the roles of the tryptophan and arginine residues in the activity of SPase I using chemical modification and site-directed mutagenesis (*7*, *22*, *24*). The results indicated that $Trp^{300}$ and some ($Arg^{77}$, $Arg^{222}$, $Arg^{315}$ and $Arg^{318}$) of the arginine residues are important for the activity. However, these residues are located fairly apart from the active site and are not directly involved in the catalytic machinery (*17*), although the P7 residue of a substrate was reported to come in close proximity to the $Trp^{300}$ by a modelling study (*17*). They were thus assumed to be important to maintain the active conformation of the enzyme. Interestingly, many of these residues reside in the C-terminal region of the enzyme.

*To whom correspondence should be addressed. Fax: +81 78 3825419, E-mail: parksj@med.kobe-u.ac.jp
†Correspondence may also be addressed. Fax: +81 49 2978168, E-mail: kenjitak@ls.toyaku.ac.jp

 

As a continuation of these studies, we investigated in the present study the effects of mutations in the C-terminal region including amino acid residues at positions from 319 to 323, which sits behind the active site region (*17*) by deletions and site-directed mutagenesis. The results thus obtained strongly suggest that $Ile^{322}$ is also important for maintaining the proper and critical local conformation of the structure backing up the active site of SPase I.

## MATERIALS AND METHODS

*Bacterial Strains, Expression Plasmids, and Other Materials—Escherichia coli* strain MV1190 was used as a host for the expression vector pT7-7 as well as for the overproduction of the wild-type and mutant proteins. The pT7-7 plasmid that has the T7 promoter and the M13 phage mGP1-2 plasmid carrying the T7 polymerase gene were obtained by Dr S. Tabor (*25*). The plasmid pT7-7/*lep* was used for overproduction of SPase I in *E. coli* MV1190 as described previously (*7*). *Escherichia coli* strain IT41 encoding a chromosomal temperature-sensitive SPase I was a gift from Dr Y. Nakamura (*26*). Restriction endonucleases, DNA amplification reagents and Tag DNA polymerase were purchased from Toyobo (Tokyo, Japan) and the T4 DNA ligation kit was obtained from Takara (Kyoto, Japan). The reagents for DNA sequencing were from GE Healthcare (Foster city, CA, USA). All other reagents used were of analytical grade and obtained from Wako Pure Chem. Industries (Osaka, Japan).

*Mutagenesis and Enzyme Purification*—DNA manipulations were carried out as described by Sambrook *et al.* (*27*). Mutagenesis was performed according to the procedure of Kunkel (*28*). Mutations were confirmed by DNA sequencing. Each of the mutated genes was inserted back into the corresponding protein gene of the pT7-7/lep expression vector (*7*). The mutant enzymes were expressed and purified as described previously (*7*, *22*).

*In Vitro and In Vivo SPase I Activity Assay*—To determine the enzymatic activity of the mutant enzymes *in vitro*, we used the chemically synthesized peptide substrate (FSASALAKI) corresponding to part of the maltose-binding protein precursor containing the cleavage site (A/K) by SPase I. In the routine assay, a 10 μl aliquot of each enzyme was added to 40μl of substrate at a final concentration of 0.4 mM in 25 mM sodium phosphate buffer, pH 7.7. The reaction was allowed to proceed at 37°C for 30 min, and stopped by the addition of 50 μl of 0.1% trifluoroacetic acid, and the reaction mixture was subsequently analysed by HPLC using a $C_{18}$ column as described previously (*7*). The activity of SPase I *in vivo* was determined using the temperature-sensitive *E. coli* SPase I strain IT41 (*26*). Measurement of SPase I activity *in vivo* was performed as described previously (*22*).

*Kinetic Study*—Kinetic parameters ($k_{cat}$, $K_m$ and $k_{cat}/K_m$) for the synthetic substrate (FSASALA/KI) were determined as described previously (*22*). The reaction was initiated by the addition of each mutant enzyme to a substrate solution containing 25 mM sodium phosphate buffer, pH 7.7. The reactions were carried out at 37°C at six or more different initial substrate concentrations (0.04–0.8 mM). The enzyme concentration used in kinetic experiments was 1.69 μM.

*Determination of Thermostability*—To test the thermostability, the wild-type and mutant enzymes in 10 mM potassium phosphate buffer, pH 7.0, containing 0.1% Lubrol PX, 10% glycerol and 35 mM NaCl were incubated at the indicated temperatures for 1 h. Remaining activities were measured by mixing 10 μl of each heat-treated enzyme with 40 μl of the synthetic substrate solution. The reaction was allowed to proceed at 37°C for 30 min and was stopped by the addition of 50 μl of 0.1% trifluoroacetic acid. Then the reaction mixture was analysed by HPLC as described previously (*7*).

*Circular Dichroism Spectroscopy*—The circular dichroism (CD) spectra of the wild-type enzyme and its mutants were recorded at a protein concentration of 2.0 μM in 25 mM sodium phosphate buffer, pH 7.7, containing 0.1% Lubrol PX and 10% glycerol with a Jasco J-720 spectropolarimeter at room temperature using the water-jacketed quartz cell with a light path of 1 mm. The sample solutions were prepared by appropriately diluting the solutions of the enzyme with 25 mM sodium phosphate buffer, pH 7.7, just before measurement. For all measurements, 1.0 nm bandwidth and 1.0 s time constant were used, and 32 scans were repeated from 200 to 250 nm at the speed of 50 nm/min with 0.1 nm/point resolution. The protein concentrations of the mutants used for CD spectroscopy were determined by amino acid analysis after acid hydrolysis.

*Alignment of the Amino Acid Sequences of SPases I*—The amino acid sequences of SPases I from various bacteria were aligned using the program ClustalW (*29*).

## RESULTS AND DISCUSSION

To investigate the roles of the C-terminal region in *E. coli* SPase I, we constructed three C-terminally truncated mutants and two kinds of site-directed mutants: SPC1 (Δ323), SPC3 (Δ321–323), SPC5 (Δ319–323), I322A and *I319A*. All mutants were expressed in *E. coli* MV1190 successfully and were purified to homogeneity. Figure 1 shows that the protein expression efficiency of the mutants in *E. coli* MV1190 was similar to that of the wild-type enzyme. All the expressed mutants were purified by successive column chromatographic procedures using DEAE-cellulose, Mono P and Sephadex G-75 as described previously (*7*). All the purified mutant enzymes were homogeneous, giving a single band on SDS–PAGE at the position corresponding to an apparent molecular mass of 37 kDa, identical with that of the wild-type enzyme (Fig. 1B). In each case, the mutant enzyme was produced in the amount of 0.2–1.5 mg per 1 l of the LB broth (Table 1).

The enzymatic activities of the mutant enzymes were determined using a synthetic substrate (FSASALA/KI) (Table 1). The mutant enzyme SPC1 (Δ323) retained full catalytic activity. In contrast, SPC3 (Δ321–323) and SPC5 (Δ319–323) exhibited activities that were only about 12% and 4%, respectively, of that of the wild-type enzyme. Furthermore, the replacement of $Ile^{322}$ or $Ile^{319}$ with alanine also significantly decreased the specific activities. Especially, the mutation of $Ile^{322}$ to alanine resulted in

84% loss of activity. We also measured the activity of all mutant enzymes using the *in vivo* assay (Table 1). In this assay, the three mutants, SPC3, SPC5 and I322A, were shown to have practically no activity, whereas I319A retained the activity. These results indicate that $Ile^{322}$ is somehow important for the enzyme activity but that $Ile^{319}$ is not so important as $Ile^{322}$.

The kinetic parameters ($k_{cat}$, $K_m$ and $k_{cat}/K_m$) of the wild-type and all mutant enzymes were determined by the *in vitro* assay using the synthetic substrate described above (Table 2). The $k_{cat}$ and $k_{cat}/K_m$ values decreased roughly in parallel with the relative activities by mutation, but it is notable that the $K_m$ values of SPC3 and I322A were elevated by 1.6-fold and 2.3-fold, respectively, as compared with that of the wild-type enzyme.

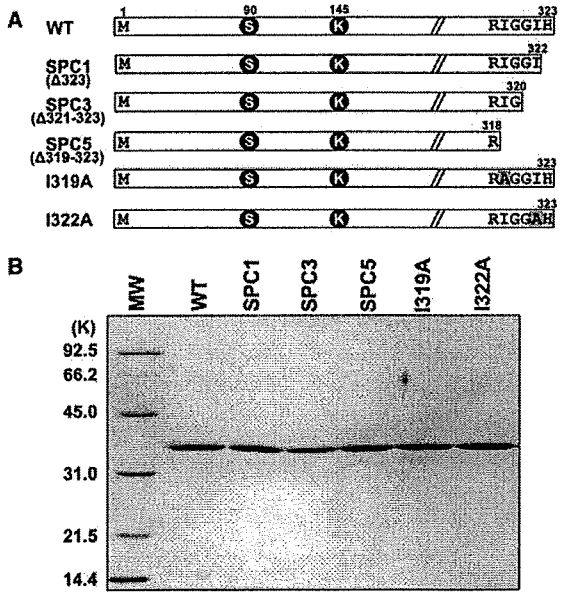


Fig. 1. **Schematic diagram and SDS-PAGE of the SPase I mutants.** (A) A schematic view of the deletion and point mutations in *E. coli* SPase I. Two active sites ($S^{90}$ and $K^{145}$) are also shown. (B) SDS-PAGE of the mutant enzymes performed on a 12.5% polyacrylamide gel under reducing conditions followed by the Coomassie brilliant blue staining. MW, molecular weight markers.

These results suggest that the deletion or mutation to Ala of $Ile^{322}$ significantly reduces not only the catalytic efficiency but also the substrate-binding affinity of the enzyme. As compared with the wild-type enzyme, I322A showed a lower $k_{cat}$ value and a higher $K_m$ value, whereas SPC5 had a lower $k_{cat}$ value, but a similar $K_m$ value. The reason for this difference is not clear at present; the deletion of the C-terminal five-residue peptide (IGGIH) might somehow favour the substrate binding as compared with SPC3 and I322A. It is tempting to assume that the newly formed C-terminal carboxyl group of $Arg^{318}$ might effectively interact with some other residue in the enzyme.

Far-UV CD spectrum was measured to compare the secondary structures of the SPase I mutants with the wild-type enzyme. As shown in Fig. 2, the CD spectra of the mutant enzymes were roughly similar to that of the wild-type enzyme. These results indicated that no gross misfolding or changes in the secondary structure of the enzymes occurred through the mutations. Figure 3 shows the thermostability profiles of the mutant enzymes. After the enzymes were incubated in 25 mM sodium phosphate buffer, pH 7.7, at various temperatures for 60 min, the remaining activities were assayed. The thermostability was significantly decreased for all the mutants except SPC3. Especially notable is the decrease in thermostability of I322A; the $T_m$ value of I322A was about 5°C lower than that of the wild-type enzyme. This suggests that $Ile^{322}$ is important for the conformational stability of the enzyme. SPC3 was apparently more thermostable than the wild-type enzyme; the reason for this result is not certain at present.

Table 2. **Kinetic parameters for SPase I mutants.**

| Enzyme | $k_{cat}$ ($h^{-1}$) | $K_m$ (mM) | $k_{cat}/K_m$ ($h^{-1}$ $mM^{-1}$) |
|---|---|---|---|
| Wild-type | 86.4 | 0.52 | 166.2 |
| SPC1 | 56.6 | 0.56 | 101.1 |
| SPC3 | 20.0 | 0.83 | 24.1 |
| SPC5 | 5.3 | 0.65 | 8.2 |
| I322A | 26.2 | 1.20 | 21.9 |
| I319A | 47.1 | 0.60 | 78.4 |

The initial rates were determined at 37°C in 25 mM sodium phosphate, pH 7.7. The concentration of the synthetic peptide (FSASALA/KI) was varied in the range of 0.04–0.8 mM. The kinetic data were analysed by double-reciprocal plots.

Table 1. **Enzymatic activities of SPase I mutants.**

| Enzyme | Mutation site | Relative enzyme amount produced | *In vitro* assay | | *In vivo* assay |
|---|---|---|---|---|---|
| | | | Specific activity (units/mg) | Relative activity (%) | Cell viability |
| Wild-type | | 1.00 | 12,800±130 | 100±1 | Yes |
| SPC1 | Δ323 | 0.95 | 11,263±450 | 87±4 | Yes |
| SPC3 | Δ321–323 | 0.15 | 1,574±330 | 12±3 | No |
| SPC5 | Δ319–323 | 0.25 | 550±640 | 4±5 | No |
| I322A | $Ile^{322}$→Ala | 0.97 | 2,048±150 | 16±1 | No |
| I319A | $Ile^{319}$→Ala | 0.90 | 6,244±900 | 49±7 | Yes |

The activities were determined by measuring the initial rates of the substrate hydrolysis. One unit is defined as the activity hydrolysing 1 pmol synthetic peptide/min. The relative activity in the *in vivo* assay was estimated from the increase in absorbance at 600 nm of *E. coli* IT41/pGP1-2 encoding each mutant enzyme relative to that encoding the wild-type enzyme. Values are means±SD, generally based on at least five independent determinations ($n \geq 5$).

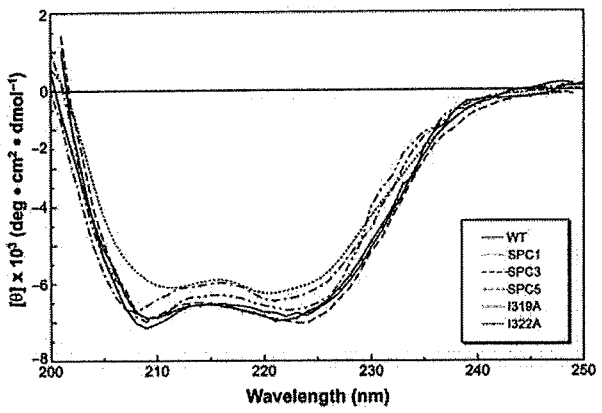


Fig. 2. **Far-UV CD spectra of the SPase I mutants.** The CD spectra of the wild-type enzyme and its mutants were recorded at a protein concentration of 2.0 μM in 25 mM sodium phosphate buffer, pH 7.7, containing 0.1% Lubral PX and 10% glycerol with a Jasco J-720 spectropolarimeter at room temperature using the water-jacketed quartz cell with a light path of 1 mm. The sample solutions were prepared by appropriately diluting the solutions of the enzyme with 25 mM sodium phosphate buffer, pH 7.7, just before measurement. For all measurements, 1.0 nm bandwidth and 1.0 s time constant were used, and 32 scans were repeated from 200 to 250 nm at the speed of 50 nm/min with 0.1 nm/point resolution. The protein concentrations of the mutants used for CD spectroscopy were determined by amino acid analysis after acid hydrolysis.

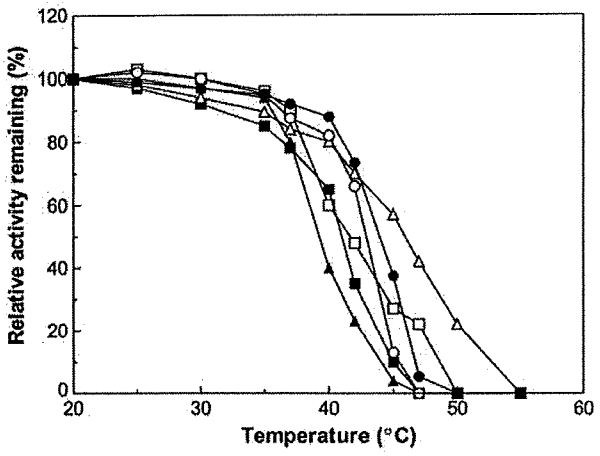


Fig. 3. **Thermostability of the SPase I mutants.** The wild-type and mutant enzymes in 10 mM potassium phosphate, pH 7.0, containing 0.1% Lubrol PX, 10% glycerol and 35 mM NaCl were incubated at the indicated temperatures for 1 h. Remaining activities were measured by mixing 10 μl of each heat-treated enzyme with 40 μl of the synthetic substrate solution. The reaction was allowed to proceed at 37°C for 30 min and was stopped by the addition of 50 μl of 0.1% trifluoroacetic acid. Then the reaction mixture was analysed by HPLC as described previously (*7*). Wild-type (solid circle); *SPC1* (open circle); *SPC3* (open triangle); *SPC5* (open square); *I319A* (solid square); *I322A* (solid triangle).

In the three-dimensional structure (Fig. 4) (*17*), $Ile^{322}$ is suggested to interact with the side chain of $Leu^{95}$. The distance between the $C\gamma^2$ atom of $Ile^{322}$ and the $C\delta^2$ atom of $Leu^{95}$ is 3.68 Å. The side chain of $Leu^{95}$ can also interact with that of $Met^{91}$ neighbouring to the catalytic $Ser^{90}$. The distance between Cβ atoms of $Leu^{95}$ and $Met^{91}$ is 3.97 Å. Therefore, the lack of the interaction with $Leu^{95}$ due to the mutation of $Ile^{322}$ may cause a local conformational change of the catalytic $Ser^{90}$ through the reorientation of $Met^{91}$. On the other hand, the side chain of $Ile^{319}$ protrudes outside the enzyme molecule and does not interact with any group near the active site (Fig. 4). Thus, the mutation of $Ile^{319}$ may cause less effect on the local conformation near the active site of the SPase I and hence its enzymatic activity (Table 1).

Figure 5 shows an alignment of the 14-residue amino acid sequences in the C-terminal regions of the 57 proteobacteria SPases I thus far available which correspond to the C-terminal 14-residue sequence of *E. coli* SPase I. As is clear from this figure, the residue $Ile^{322}$ of *E. coli* SPase I is well conserved in many proteobacteria except that it is partially replaced with bulky hydrophobic amino acids such as Phe, Leu, Val and Trp. Furthermore, this homology appears to extend to other bacteria (data not shown). On the other hand, the residue $Ile^{319}$ of *E. coli* is less conserved than $Ile^{322}$ and even partially replaced with non-hydrophobic amino acids. These results are thus consistent with the supposition obtained above. Incidentally, it may be worthy of note that the residue $Arg^{318}$ of *E. coli* SPase I, which was previously deduced to be one of the few important Arg residues in the

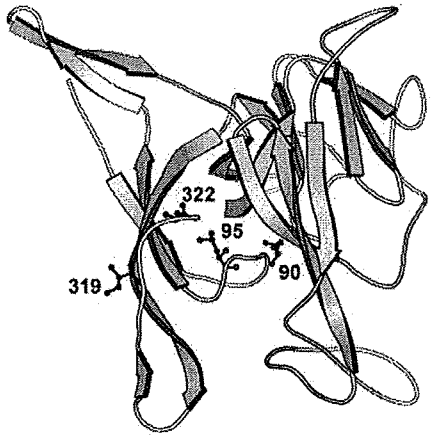


Fig. 4. **Schematic representation of the backbone conformation of SPase I.** The side chains of $Ile^{319}$ and $Ile^{322}$ (black), and $Ser^{90}$ and $Leu^{95}$ (grey) are drawn by the ball-and-stick model. The structure was presented from the PDB atomic coordinates 1B12 (*16*) with a slight modification using the program MolScript (*30*).

enzyme (*24*), is also highly conserved in the SPases I of other bacteria (Fig. 5).

$Ile^{322}$ (this study), $Trp^{300}$ (*22*) and some Arg residues including $Arg^{318}$ (*24*) are located fairly apart from the active site of SPase I and are not directly involved in the catalytic machinery. Their mutations, however, resulted in a great loss of enzymatic activity, indicating that

| | | | |
|---|---|---|---|
| | * | | * |
| *Escherichia coli* (NP_417063) | WPTGLRLSRIGGIH | *Helicobacter pylori* (NP_223241) | RYLVRWERMFKSVE |
| *Shigella flexneri* (NP_708420) | WPTGVRLSRIGGIH | *Helicobacter pylori* (NP_207371) | RYLVRWERMFKSVG |
| *Salmonella enterica* (NP_457111) | WPTGVRLSRIGGIH | *Wolinella succinogenes* (NP_907517) | DYKIRWNRIGKSIE |
| *Yersinia pestis* (NP_406234) | WPTGVRLSRIGGIH | *Campylobacter jejuni* (NP_282017) | DKNVRWERIGRFVD |
| *Yersinia enterocolitica* (AAQ11415) | WPTGVRLSRIGGIH | *Rickettsia rickettsii* (NP_00153218) | LKPWVESVRLNRIF |
| *Erwinia carotovora* (YP_051368) | WPTGVRLSRIGGIH | *Rickettsia conorii* (NP_359793) | LKPWIESVRLNRIF |
| *Photorhabdus luminescens* (NP_930561) | WPTGVRFSRIGGIN | *Rickettsia sibirica* (NP_00142370) | LKPWIESVRLNRIF |
| *Vibrio cholerae* (NP_232091) | IPTGVRFNRVGGIH | *Rickettsia prowazekii* (NP_220508) | LKPWIESVRLSRIF |
| *Vibrio parahaemolyticus* (NP_798952) | IPTGVRFNRIGGIH | *Bradyrhizobium japonicum* (NP_771702) | FWRWPWAVRWNRFF |
| *Vibrio vulnificus* (NP_760461) | IPTGVRFNRIGGIH | *Rhodopseudomonas palustris* (NP_948038) | IWRWPTAVRWGRIF |
| *Buchnera aphidicola* (NP_240083) | WPTGIRINRIGSIH | *Magnetospirillum magnetotac* (ZP_00048501) | LWRWPTDVRWNRIF |
| *Buchnera aphidicola* (NP_660598) | WPTGIRIKRIGNIY | *Magnetospirillum magnetotac* (ZP_00051050) | VWRWPWAIRYARLL |
| *Buchnera-aphidicola* (NP_777862) | WPTGIQFDRIGNIY | *Brucella suis* (NP_697674) | WPTDVRFNRLFTWV |
| *Candidatus Blochmannia florida* (NP_878820) | WPTGIKLDRIGMLK | *Mesorhizobium loti* (NP_108011) | IWKWPSLWRVSRLF |
| *Haemophilus influenzae* (ZP_00157522) | PTGFRFERFFTAIK | *Bartonella henselae* (NP_033344) | IWRWPFDVRWNRLF |
| *Haemophilus influenzae* (NP_438188) | PTGFRFERFFTAIK | *Bartonella quintana* (NP_032107) | IWRWPFDVRWNRLF |
| *Haemophilus influenzae* (ZP_00154746) | PTGFRFDRFFTAIK | *Sinorhizobium meliloti* (NP_385177) | IWKWPANLRYDRLF |
| *Haemophilus somnus* (ZP_00133139) | PKGIRFSRMFTSIK | *Bradyrhizobium japonicum* (NP_767807) | WTCAATGFRLARFF |
| *Actinobacillus pleuropneumo* (ZP_00134799) | PSGLRFDRMFTSIN | *Bradyrhizobium* (NP_767807) | VWTWLSGFRLARFF |
| *Pseudomonas aeruginosa* (NP_249459) | MSNLPNFSRVGVIH | *Rhodopseudomona palustris* (NP_946177) | VTDWFSGFRVARFF |
| *Pseudomonas fluorescens* (P26844) | LSHLPNFSRVGLIK | *Serratia marcescens* (NP_941103) | TDHSWDSRFWGTVK |
| *Burkholderia pseudomallei* (YP_109022) | WWNFSDLKRIGSFN | *Salmonella typhi* (NP_058Z22) | TDHSWDSRFWGPVK |
| *Ralstonia solanacearum* (NP_519182) | WWNLGDWKRIGSFH | *Bradyrhizobium japonicum* (NP_772268) | HLVGKVTRIFWSLD |
| *Azoarcus* (YP_160177) | WFNFSDWKRIGGFH | *Desulfotalea psychrophila* (YP_063843) | RWTSIKWARIGRLV |
| *Bordetella bronchiseptica* (NP_890282) | WWNFSDLSRIGRFH | *Neisseria meningitidis* (NP_283755) | WNFGDFGRAGTAIR |
| *Bordetella parapertussis* (NP_885463) | WWNFSDLSRIGRFH | *Ralstonia solanacearum* (NP_519837) | WYLPRLARIGRPLD |
| *Bordetella pertussis* (NP_881060) | WWNFSDLSRIGRFH | *Magnetospirillum magnetotac* (ZP_00051050) | GLLVPPAPRRVPVH |
| *Nitrosomonas europaea* (NP_842323) | WNFNDLSRIGTLIK | *Proteus vulgaris* (NP_640175) | GHSDKELTRTGIIP |
| *Acinetobacter* (YP_047167) | GFKIPSFNRNGTID | | |

Fig. 5. **Alignment of the C-terminal 14-residue sequence of *E. coli* SPase I with the corresponding sequences of SPases I from other proteobacteria.** The accession number is given in parenthesis. Asterisk denotes the residues corresponding to $Ile^{322}$ in *E. coli* SPase I.

certain amino acid residues away from the active site may contribute significantly to the active conformation, hence the activity of the enzyme. These results thus constitute an example of the impact of non-active site mutation in enzyme. Similar results may be obtained with other enzymes. Indeed, non-active site amino acid substitutions were reported to be the major factors leading to the decreases in inhibitor binding to the HIV-1 protease (*31*).

This work was supported in part by a Grant-in-Aid for Scientific Research from the Ministry of Education, Culture, Sports, Science and Technology to Y.K. (11760077).

## REFERENCES

1. Wickner, W., Driessen, A.J.M., and Hartl, F.-U. (1991) The enzymology of protein translocation across the *Escherichia coli* plasma membrane. *Annu. Rev. Biochem.* **60**, 101–124
2. Wolfe, P.B., Wickner, W., and Goodman, J.M. (1983) Sequence of the leader peptidase gene of *Escherichia coli* and the orientation of leader peptidase in the bacterial envelope. *J. Biol. Chem.* **258**, 12073–12080
3. Paetzel, M., Dalbey, R.E., and Strynadka, N.C.J. (2000) The structure and mechanism of bacterial type I signal peptidases, A novel antibiotic target. *Pharmacol. Ther.* **87**, 27–49
4. Chang, C.N., Blobel, G., and Model, P. (1978) Detection of prokaryotic signal peptidase in an *Escherichia coli* membrane fraction: endoproteolytic cleavage of nascent f1 pre-coat protein. *Proc. Natl. Acad. Sci. USA* **75**, 361–365
5. Date, T. and Wickner, W. (1981) Isolation of the *Escherichia coli* leader peptidase gene and effects of leader peptidase overproduction *in vivo*. *Proc. Natl. Acad. Sci. USA* **78**, 6106–6110
6. Dalbey, R.E. and Wickner, W. (1985) Leader peptidase catalyzes the release of exported proteins from the outer surface of the *Escherichia coli* plasma membrane. *J. Biol. Chem.* **260**, 15925–15931
7. Kim, Y.-T., Muramatsu, T., and Takahashi, K. (1995) Leader peptidase from *Escherichia coli*: overexpression, characterization, and inactivation by modification of tryptophan residues 300 and 310 with *N*-bromosuccinimide. *J. Biochem.* **117**, 535–544
8. Zwizinski, C. and Wickner, W. (1980) Purification and characterization of leader (signal) peptidase from *Escherichia coli*. *J. Biol. Chem.* **255**, 7973–7977
9. Wolfe, P.B., Silver, P., and Wickner, W. (1982) The isolation of homogeneous leader peptidase from a strain of *Escherichia coli* which overproduces the enzyme. *J. Biol. Chem.* **257**, 7898–7902
10. Tschantz, W.R., Sung, M., Delgodo-Partin, V.M., and Dalbey, R.E. (1993) A serine and a lysine residue implicated in the catalytic mechanism of the *Escherichia coli* leader peptidase. *J. Biol. Chem.* **268**, 27349–27354
11. van Heijne, G. (1983) Patterns of amino acids near signal-sequence cleavage sites. *Eur. J. Biochem.* **133**, 17–21
12. Moore, K.E. and Miura, S. (1987) A small hydrophobic domain anchors leader peptidase to the cytoplasmic membrane of *Escherichia coli*. *J. Biol. Chem.* **262**, 8806–8813
13. Bilgin, N., Lee, J.I., Zhu, H., Dalbey, R.E., and von Heijne, G. (1990) Mapping of catalytically important domains in *Escherichia coli* leader peptidase. *EMBO J.* **9**, 2717–2722
14. Zimmermann, R., Watts, C., and Wickner, W. (1982) The biosynthesis of membrane-bound M13 coat protein. *J. Biol. Chem.* **257**, 6529–6536
15. Kuo, D.W., Chan, H.K., Wilson, C.J., Griffin, P.R., Williams, H., and Knight, W.B. (1993) *Escherichia coli*

leader peptidase: production of an active form lacking a requirement for detergent and development of peptide substrates. *Arch. Biochem. Biophys.* **303**, 274–280
16. Paetzel, M., Dalbey, R.E., and Strynadka, N.C.J. (1998) Crystal structure of a bacterial signal peptidase in complex with a β-lactam inhibitor. *Nature* **396**, 186–190
17. Paetzel, M., Dalbey, R.E., and Strynadka, N.C.J. (2002) Crystal structure of a bacterial signal peptidase apoenzyme: implications for signal peptide binding and the Ser-Lys dyad mechanism. *J. Biol. Chem.* **277**, 9512–9519
18. Sung, M. and Dalbey, R.E. (1992) Identification of potential active-site residues in the *Escherichia coli* leader peptidase. *J. Biol. Chem.* **267**, 13154–13159
19. Black, M.T. (1993) Evidence that the catalytic activity of prokaryote leader peptidase depends upon the operation of a serine-lysine catalytic dyad. *J. Bacteriol.* **175**, 4957–4961
20. Paetzel, M., Strynadka, N.C., Tschantz, W.R., Casareno, R., Bullinger, P.R., and Dalbey, R.E. (1997) Use of site-directed chemical modification to study an essential lysine in *Escherichia coli* leader peptidase. *J. Biol. Chem.* **272**, 9994–10003
21. Black, M.T., Munn, J.G.R., and Allsop, A.E. (1992) On the catalytic mechanism of prokaryotic leader peptidase I. *Biochem. J.* **282**, 539–543
22. Kim, Y.-T., Muramatsu, T., and Takahashi, K. (1995) Identification of Trp300 as an important residue for *Escherichia coli* leader peptidase activity. *Eur. J. Biochem.* **234**, 358–362
23. Kuo, D., Weidner, J., Griffin, P., Shah, S.K., and Knight, W.B. (1994) Determination of the kinetic parameters of *Escherichia coli* leader peptidase activity using a continuous assay: the pH dependence and time-dependent inhibition by β-lactams are consistent with a novel serine protease mechanism. *Biochemistry* **33**, 8347–8354
24. Kim, Y.-T., Kurita, R., Kojima, M., Nishii, W., Tanokura, M., Muramatsu, T., Ito, H., and Takahashi, K. (2004) Identification of arginine residues important for the activity of *Escherichia coli* signal peptidase I. *Biol. Chem.* **385**, 381–388
25. Tabor, S. (1990) Expression using the T7 RNA polymerase/promoter system in *Current Protocols in Molecular Biology* (Ausubel, FM., Brent, R., Kingston, R.E., Moore, D.D., Seidman, J.G., Smith, J.A., and Struhl, K., eds.) pp. 16. 2. 1–16. 2. 11 Greene Publishing and Wiley Interscience, New York
26. Inada, T., Court, D.L., Ito, K., and Nakamura, Y. (1989) Conditionally lethal amber mutations in the leader peptidase gene of *Escherichia coli*. *J. Bacteriol.* **171**, 585–587
27. Sambrook, J., Fritsch, E.F., and Maniatis, T. (1989) *Molecular Cloning: A Laboratory Manual,* 2nd edn, Cold Spring Harbor Laboratory, Cold Spring Harbor, NY
28. Kunkel, T.A. (1985) Rapid and efficient site-specific mutagenesis without phenotypic selection. *Proc. Natl. Acad. Sci. USA* **82**, 488–492
29. Thompson, J.D., Higgins, D.G., and Gibson, T.J. (1994) CLUSTAL W: improving the sensitivity of progressive multiple sequence alignment through sequence weighting, position-specific gap penalties and weight matrix choice. *Nucleic Acids Res.* **22**, 4673–4680
30. Kraulis, P.J. (1991) MOLSCRIPT: a program to produce both detailed and schematic plots of protein structures. *J. Appl. Crystallogr.* **24**, 946–950
31. Olsen, D.B., Stahlhut, M.W., Rutkowsky, C.A., Schock, H.B., vanOlden, A.L., and Kuo, L.C. (1999) Non-active site changes elicit broad-based cross-resistance of the HIV-1 protease to inhibitors. *J. Biol. Chem.* **274**, 23699–23701